

1 An optimized tracer-based approach for estimating organic carbon emissions from
2 biomass burning in Ulaanbaatar, Mongolia

3
4 Jayant Nirmalkar¹, Tsatsral Batmunkh², Jinsang Jung^{1,*}

5 ¹Center for Gas Analysis, Korea Research Institute of Standards and Science
6 (KRISS), Daejeon 34113, Republic of Korea

7 ²Department of Green Development Policy and Planning,
8 Ministry of Environment and Tourism, Ulaanbaatar-15160, Mongolia

9
10
11 *Correspondence to: Jinsang Jung (jsjung@kriss.re.kr)*

13 Abstract

14 The impact of biomass burning (BB) on atmospheric particulate matter of $<2.5 \mu\text{m}$
15 diameter ($\text{PM}_{2.5}$) at Ulaanbaatar, Mongolia, was investigated using an optimized tracer-
16 based approach during winter and spring, 2017. Integrated 24 h $\text{PM}_{2.5}$ samples were
17 collected on quartz fiber filters using a 30 L min^{-1} air sampler at an urban site in
18 Ulaanbaatar. The aerosol samples were analyzed for organic carbon (OC) and elemental
19 carbon (EC), anhydrosugars (levoglucosan, mannosan, and galactosan), and water-
20 soluble ions. OC was found as the predominant species, contributing 64% and 56% to
21 the quantified aerosol components in $\text{PM}_{2.5}$ in winter and spring, respectively. BB was
22 identified as a major source of $\text{PM}_{2.5}$, followed by dust and secondary aerosols.
23 Levoglucosan/mannosan and levoglucosan/ K^+ ratios indicate that BB in Ulaanbaatar
24 was mainly originated from burning of softwood. Because of the large uncertainty
25 associated with quantitative estimation of OC emitted from BB (OC_{BB}), a novel
26 approach was developed to optimize the OC/levoglucosan ratio for estimating OC_{BB} .
27 The optimum OC/levoglucosan ratio in Ulaanbaatar was obtained by regression analysis
28 between $\text{OC}_{\text{non-BB}}$ ($\text{OC}_{\text{total}} - \text{OC}_{\text{BB}}$) and levoglucosan concentrations that gives the lowest
29 coefficient of determination (R^2) and slope. The optimum OC/levoglucosan ratio was
30 found to be 27.6 and 18.0 for winter and spring, respectively, and these values were
31 applied in quantifying OC_{BB} . It was found that 68% and 63% of the OC were emitted
32 from BB during winter and spring, respectively. This novel approach can also be
33 applied to other study sites to quantify OC_{BB} using their own chemical measurements.
34 In addition to OC_{BB} , sources of $\text{OC}_{\text{non-BB}}$ were also investigated through multivariate
35 correlation analysis. It was found that $\text{OC}_{\text{non-BB}}$ was originated mainly from coal burning,
36 vehicles, and vegetative emissions.

37

38 **Keywords:** Source identification, Biomass burning, Optimized organic-
39 carbon/levoglucosan ratio

40 **1. Introduction**

41 Organic aerosol (OA) contributes a significant fraction (10%–90%) of atmospheric
42 particulate matter (PM), which can affect human health and air quality (Jimenez et al.,
43 2009; Maenhaut et al., 2011; Fu et al., 2012; Allan et al., 2014; Chen et al., 2018). An
44 understanding of the sources of PM is highly relevant for air-quality remediation.
45 Biomass burning (BB) is a major source of organic carbon (OC) in PM_{2.5} (PM with
46 aerodynamic diameter ≤ 2.5 μm) and it may become more significant in the future as air-
47 quality regulations restrict other anthropogenic emissions (Davy et al., 2011; Allan et al.,
48 2014; Sullivan et al., 2019). Coal combustion, thermal power plants, and traffic
49 emissions also make potential contributions to the OC content of PM (Watson et al.,
50 2001a, b; Pei et al., 2016; Deshmukh et al., 2019; Haque et al., 2019), modifying PM
51 characteristics such as hygroscopicity, light-attenuating properties, and health impacts
52 (Jung et al., 2009; Sullivan et al., 2019). Previous studies have observed that the toxicity
53 of PM_{2.5} increases with the oxidation potential of BB species because of the water-
54 soluble fraction of OC (Verma et al., 2014).

55 Previous studies have identified and quantified OC emitted from BB (OC_{BB}) using
56 the BB tracers (levoglucosan, mannosan, galactosan, and K⁺). Levoglucosan is
57 produced from the pyrolysis of cellulose at temperatures of $>300^\circ\text{C}$ (Simoneit et al.,
58 1999; Claeys et al., 2010; Maenhaut et al., 2011; Nirmalkar et al., 2015; Achad et al.,
59 2018); and two isomers of levoglucosan, mannosan and galactosan are produced by the
60 burning of hemicellulose (Reche et al., 2012). The atmospheric concentration of
61 levoglucosan is higher than that of the two isomers because of the lower content of
62 hemicellulose (20%–30%, dry weight) than cellulose (40%–50%) in softwood and
63 hardwood (Reche et al., 2012; Sharma et al., 2015). Water-soluble K⁺ can also be used

64 as a BB tracer (Pio et al., 2008; Cheng et al., 2013; Nirmalkar et al., 2015; Chen et al.,
65 2018; Chantara et al., 2019). The proportion of these BB tracers in PM depends on
66 various factors such as the type of biomass (softwood, hardwood, crop, grass, etc.),
67 where it is burnt (traditional stoves, fireplaces, field burning, burning in closed
68 chambers, etc.), the type of burning (smoldering, flaming, etc.), and the burning season
69 (Fu et al., 2012; Cheng et al., 2013; Jung et al., 2014). Levoglucosan/mannosan,
70 levoglucosan/K⁺, and OC/levoglucosan ratios were used to identify major biomass types
71 and quantify OC_{BB} (Reche et al., 2012; Cheng et al., 2013; Jung et al., 2014; Chen et al.,
72 2018). However, OC/levoglucosan ratios are quite variable even with the same type of
73 BB because of variations in burning type, place, and season (Cheng et al., 2013;
74 Thepnuan et al., 2019 and references therein). It is therefore essential to optimize the
75 OC/levoglucosan ratio to better estimate OC_{BB}.

76 Ulaanbaatar, with a population of about 1 million, is an atmospheric pollution
77 ‘hotspot’ because of its topography, being situated in the Tuul river valley and
78 surrounded by the Khentei mountains, with a high elevation (1300 m–1949 m above sea
79 level) and large variations in temperature (–28°C to +16°C) and relative humidity
80 (17.7%–72.7%; Table 1; Batmunkh et al., 2013; Jung et al., 2014). As the world’s
81 coldest capital city during winter, it requires additional fuel for space heating. The
82 topography and low-temperature conditions cause an increase in PM concentrations,
83 which are exacerbated by low wind speeds and atmospheric temperature inversions
84 (Jung et al., 2010).

85 Half of the residents in Ulaanbaatar lives in 160,000 Gers (traditional Mongolian
86 dwellings) (Guttikunda and Jawahar, 2014). Biomass is used as fuel for cooking and
87 heating in many of low-income Gers at Ulaanbaatar. The common tree species in

88 Mongolia are larch, pine, cedar, spruce, birch; these are mostly softwood
89 (<http://www.fao.org/3/w8302e/w8302e05.htm>; <http://www.fao.org/3/a-am616e.pdf>,
90 excess date 17-12-2019). Each Ger burns an average of 3 m³ of wood per year
91 (Guttikunda, 2008; Zhamsueva et al., 2018). Organic carbon (OC) has severe effects on
92 human health and global climate change (Sun et al., 2019). But there are very few
93 estimates of OC emitted from biomass burning (OC_{BB}) in Ulaanbaatar. Few studies have
94 investigated the chemical characteristics of aerosol in Ulaanbaatar (Jung et al., 2010;
95 Davy et al., 2011; Batmunkh et al., 2013), with none examining the contribution of
96 OC_{BB} and type of biomass. Therefore, this study estimated appropriate concentration of
97 OC_{BB} and identified the type of biomass at Ulaanbaatar, Mongolia.

98 In this study, we quantified the BB tracers levoglucosan, mannosan, galactosan, K⁺,
99 and other chemical species. Potential sources of PM_{2.5} were identified by principal
100 component analysis (PCA), with levoglucosan/K⁺ and levoglucosan/mannosan ratios
101 being used to identify major biomass types. OC_{BB} can be quantified from
102 OC/levoglucosan ratios and levoglucosan concentrations in PM. However, uncertainties
103 of OC_{BB} are high because OC/levoglucosan ratios can vary depending on fuel type,
104 burning conditions, and burning place (Duan et al., 2004; Cheng et al., 2013; Jung et al.,
105 2014). Therefore, it is required to determine the most suitable OC/levoglucosan ratio of
106 BB emissions for estimating appropriate concentration of OC_{BB}. Here, for the first time,
107 optimized OC/levoglucosan ratios were investigated for estimating concentrations of
108 OC_{BB} during winter and spring. OC_{non-BB} sources were also investigated using
109 multivariate correlation analysis with ions and elemental carbon (EC).

110

111 **2. Methods**

112 2.1 Sampling site and aerosol sampling

113 Aerosol sampling was carried out in Ulaanbaatar during the winter (17 January to
114 03 February) and spring (17 April to 4 May) of 2017, with 24 h periods commencing
115 daily at 11:00 local time. An aerosol sampler was installed on the rooftop of the
116 National Agency for Meteorology and Environmental Monitoring station in Ulaanbaatar
117 (47°92' N, 106°90' E, Fig. 1), 10 m above ground level. The sampling site was located
118 at 8 km–10 km far from two coal based thermal power plants to the west (Chung and
119 Chon, 2014). PM_{2.5} samples were collected on 47 mm diameter quartz fiber filters (Pall-
120 Life Sciences, USA) using an aerosol sampler (Murata Keisokuki Service, Japan) at a
121 flow rate of 30 L min⁻¹. Field blank filter was collected during winter (n=1) and spring
122 (n=1). The quartz fiber filter was loaded in the sampler for 5 minutes without operating
123 a pump. The concentration of all chemical analytes has been corrected using blank
124 filters concentration. Sampled filters were wrapped in aluminum foil and heated at
125 550°C for 12 h to remove adsorbed impurities before use and stored at -20°C before
126 and after sampling.

127

128 2.2 Filter analysis

129 A one-fourth part of each quartz fiber filter sample was extracted in 10 mL
130 ultrapure water (resistivity 18.2 MΩ, total OC content < 1 ppb,) under ultrasonication
131 for 30 min. The water extract was then filtered using a syringe filter (Millipore,
132 Millex-GV, 0.45μm) and stored at 4°C pending analysis. Water-soluble cations (K⁺,
133 Na⁺, Ca²⁺, Mg²⁺, and NH₄⁺) were quantified by an ion chromatograph (Dionex ICS
134 5000, Thermo Fisher Scientific, USA). Water-soluble cations were separated using an
135 IonPac CS-12A column (Thermo Fisher Scientific, USA) with 20 mM methanesulfonic

136 acid as eluent at a flow rate of 1.0 mL min⁻¹. Water-soluble anions (Cl⁻, NO₃⁻, and
137 SO₄²⁻) were separated using an IonPac AS-15 column (Thermo Fisher Scientific, USA)
138 with 40 mM KOH as eluent at a flow rate of 1.2 mL min⁻¹. The detection limits for
139 major inorganic ions based on 3σ of blanks were 0.01 μg m⁻³, 0.01 μg m⁻³, and 0.03 μg
140 m⁻³ for NO₃⁻, SO₄²⁻, and NH₄⁺, respectively.

141 Levoglucosan, mannosan, and galactosan were measured by a high-performance
142 anion-exchange chromatograph (Dionex, ICS-5000, Thermo Fisher Scientific, USA)
143 with pulsed amperometric detection involving an electrochemical detector with a gold
144 working electrode. Details of the method are given elsewhere (Jung et al., 2014). In
145 brief, separation involved a CarboPak MA1 (4 × 250 mm, Thermo Fisher Scientific,
146 USA) analytical column and NaOH eluent (360 mM, 0.4 mL min⁻¹). Limits of detection
147 were 3.0 ng m⁻³, 0.7 ng m⁻³, and 1.0 ng m⁻³ for levoglucosan, mannosan, and galactosan,
148 respectively.

149 Aerosol samples were analyzed for OC and EC using a thermal optical OC/EC
150 analyzer (Sunset Laboratory Inc. Forest Grove, OR, USA) with laser transmittance-
151 based correction of pyrolysis. Details of the analyzer and quality-control parameters are
152 reported elsewhere (Jung et al., 2014). In brief, 1.5 cm² punch samples of the quartz
153 fiber filter were placed in a quartz dish inside the thermal desorption oven of the
154 analyzer. OC and EC were quantified using a temperature program developed by the US
155 National Institute for Occupational Safety and Health (NIOSH) in an inert atmosphere
156 (100% He) and in an oxidizing atmosphere (98% He + 2% O₂), respectively. Detection
157 limits of OC and EC were 0.04 and 0.01 μg C m⁻³, and analytical uncertainties of them
158 were 1.3% and 3.7%, respectively.

159

160 2.3. Conditional Probability Function

161 The Conditional Probability Function (CPF) calculates the probability that a source
162 is located within a particular wind direction sector, $\Delta\Theta$:

$$163 \quad CPF = \frac{m_{\Delta\Theta}}{n_{\Delta\Theta}}$$

164 where $n_{\Delta\Theta}$ is the number of times that the wind passed through direction sector $\Delta\Theta$,
165 and $m_{\Delta\Theta}$ is the number of times that the source contribution peaked while the wind
166 passed through sector $\Delta\Theta$ (Ashbaugh et al., 1985). To use CPF with the Ulaanbaatar
167 data, the 24 h averaged source contribution data have been applied to all 1 h wind
168 direction averages recorded at the site for each date. The angular interval $\Delta\Theta$ was set at
169 10° . To calculate $m_{\Delta\Theta}$, the 75th percentiles of source contribution concentrations were
170 counted. CPF is useful in determining the direction of a source from a receptor site;
171 however, it cannot determine the actual location of the source.

172

173 2.4 Principal component analysis

174 In order to identify the source groupings of chemical species in PM_{2.5}, principal
175 component analysis (PCA) was applied. PCA is done using a commercially available
176 software package (SPSS, version 10.0). PCA applies projection dimension reduction
177 methods, converting several concentrations sets into significant sets of columns
178 (principal components, PCs) without damaging the original data. PCA is a widely used
179 statistical technique to quantitatively identify a small number of independent factors
180 among the species concentrations, which can explain the variance of the data, by using
181 the eigenvector decomposition of a matrix of pair-wise correlations. PCA with varimax
182 rotation and retention of principal components having eigenvalues >1.0 was used to

183 identify major species associated with different sources. It was widely used for
184 identification of pollution sources in the atmosphere (Fang et al., 2003, Nirmalkar et al.,
185 2015).

186

187 **3. Results and Discussion**

188 **3.1 Chemical characteristics of PM_{2.5} and source identification**

189 Mass concentrations of carbonaceous aerosol, BB tracers, and water-soluble ions in
190 PM_{2.5} samples collected at Ulaanbaatar during winter and spring of 2017 are
191 summarized in Table 1. OC contributed $64 \pm 5.1\%$ and $56 \pm 6.0\%$ of the quantified
192 aerosol components in PM_{2.5} in winter and spring, respectively (Table 1). Average
193 concentrations of OC during winter were five times those obtained in spring (Fig. 2).
194 Previously, OC has been observed as major component in PM_{2.5} in Ulaanbaatar during
195 winter period (Jung et al., 2010; Batmunkh et al., 2013). This may be attributed to
196 additional BB emission for home heating, and temperature inversions with low wind
197 speeds (average wind speed of $1.43 \pm 0.73 \text{ m s}^{-1}$; Table 1 and Fig. 3a). OC
198 concentrations decreased with increasing wind speed during winter (Fig. 3a) and spring
199 (Fig. 3b), over all air temperature ranges. The inverse relationship between OC and
200 wind speed during winter (Fig. 3a) and spring (Fig. 3b) suggests a predominance of
201 local sources, with higher wind speeds flushing air pollutants out of the area whereas
202 low wind speeds allow them to accumulate (Khan et al., 2010; Wang et al., 2018).

203 Average concentration of EC during winter ($1.71 \pm 0.58 \mu\text{g m}^{-3}$) was higher than
204 that in spring ($1.11 \pm 0.42 \mu\text{g m}^{-3}$) (Table 1), consistent with general urban observations
205 in cities of China (Ji et al., 2016) and India (Panda et al., 2016). During both winter and
206 spring, EC concentrations at the study site were lower and having different trends

207 compared to those observed in a suburban site ($2.3 \pm 1.0 \mu\text{g m}^{-3}$ and $3.1 \pm 1.5 \mu\text{g m}^{-3}$,
208 respectively) and an urban site ($2.3 \pm 1.0 \mu\text{g m}^{-3}$ and $3.3 \pm 1.2 \mu\text{g m}^{-3}$, respectively) in
209 Shanghai, China (Feng et al., 2009).

210 The potential source direction of EC during winter and spring was west as shown in
211 Fig. 5; this can be explained by the influence of emission from thermal power plants.
212 Correlation of EC was strong with Ca^{2+} during spring as shown in Fig. 4. CPF analysis
213 suggested that potential source direction of EC and Ca^{2+} was similar (Fig. 5). High
214 abundances of Ca^{2+} and EC is observed from stack emission of coal fired thermal power
215 plants (Pei et al., 2016; Zhang et al., 2015). Thus, EC and Ca^{2+} in Ulaanbaatar might be
216 strongly related to emission from thermal power plants.

217 Daily concentrations of levoglucosan, mannosan and galactosan have similar trends
218 during winter and spring (Fig. 2), possibly because of combustion of similar biomass
219 fuels in both seasons. Changes in concentrations of these BB tracers might be attributed
220 to changes in relative proportions of cellulose and hemicellulose in different biomass
221 fuels (Zhu et al., 2015; Nirmalkar et al., 2015). Concentrations of anhydrosugars were
222 four times higher in winter than in spring (Table 1) due to increased heating
223 requirements in winter. The higher relative humidity (58.5%–72.7%) and lower
224 temperature (-10.5°C to -27.8°C ; Table 1) in winter can also contribute to longer
225 atmospheric residence times due to increased levoglucosan stability (Lai et al., 2014).
226 Higher concentrations of BB tracers in winter than spring have previously been
227 observed in Beijing, China, (Liang et al., 2016) and were attributed to meteorological
228 conditions similar to those of Ulaanbaatar. Further it was observed that during winter
229 the ambient temperature was consistently low (less than -10°C , Fig. 3a) in Ulaanbaatar
230 therefore residential biomass burning occurred continuously for space heating. Thus,

231 there would be no dependence of emission rates of levoglucosan and mannosan with
232 ambient temperature during the sampling period. The concentration of levoglucosan and
233 mannosan may be influenced by local wind speed as shown in Fig. 3a rather than
234 ambient temperature. Average K^+ concentration ($0.08 \pm 0.05 \mu\text{g m}^{-3}$) in this study is
235 significantly lower than the K ($0.32 \mu\text{g m}^{-3}$) observed in Ulaanbaatar during 2004-2008
236 (Davy et al., 2011).

237 Among water-soluble ions, SO_4^{2-} ($9.7 \pm 3.4 \mu\text{g m}^{-3}$) was the most dominant $\text{PM}_{2.5}$
238 species during winter, followed by NH_4^+ ($6.2 \pm 2.4 \mu\text{g m}^{-3}$) and NO_3^- ($4.2 \pm 1.7 \mu\text{g m}^{-3}$),
239 whereas SO_4^{2-} ($1.9 \pm 0.5 \mu\text{g m}^{-3}$) was the dominant species during spring, followed by
240 Ca^{2+} ($0.9 \pm 0.4 \mu\text{g m}^{-3}$) and NH_4^+ ($0.7 \pm 0.3 \mu\text{g m}^{-3}$). The total $\text{SO}_4^{2-} + \text{NH}_4^+ + \text{NO}_3^-$
241 content accounted for 27% and 23% of the total measured chemical species during
242 winter and spring, respectively (Fig. 2 and Table 1). SO_4^{2-} is the most prevalent water-
243 soluble ion in $\text{PM}_{2.5}$ in Wuhan, Guangzhou, and Tianjin (China) due to industrial
244 emissions and coal burning (Gu et al., 2011; Tao et al., 2014; Huang et al., 2016; Pei et
245 al., 2016). This suggests that the higher SO_4^{2-} concentration in Ulaanbaatar may be
246 attributable to emissions from the three major coal-fired thermal power plants near the
247 study site.

248 The atmospheric concentrations of OC ($11\text{--}17 \mu\text{g m}^{-3}$) and levoglucosan (0.46--
249 $0.73 \mu\text{g m}^{-3}$) were higher for samples collected during 27–30 April 2017 than on almost
250 all remaining days in spring (Fig. 2b). Backward atmospheric trajectories based on the
251 Hybrid Single-Particle Lagrangian Integrated Trajectory (HYSPLIT) model provided by
252 the US National Oceanic and Atmospheric Administration (NOAA) Air Resources
253 Laboratory (ARL) indicate that during those days' air masses originated from a region
254 where a significant number of fires were detected [US Fire Information for Resource

255 Management System (FIRMS); National Aeronautics and Space Administration
256 (NASA); Fig. 6a, b)]. Thus, the elevated OC and levoglucosan concentrations during
257 27–30 April might be influenced by long-range transport of BB from north of Mongolia.

258

259 3.2 Principal Component Analysis

260 Principal component analysis (PCA) is a useful tool for reducing the dimensionality
261 of large aerosol datasets to principal components using varimax rotation for source
262 identification (Cao et al., 2005; Lin et al., 2018; Nirmalkar et al., 2019). Four principal
263 components (PCs) in winter and three in spring were identified with eigenvalues >1
264 after varimax rotation explaining 96% and 92%, respectively, of the total variance
265 (Tables 2 and 3). The PCs were categorized on the basis of loadings of chemical
266 components as follows. In winter, PC1 includes BB characterized by high loadings of
267 levoglucosan, mannosan, and galactosan; PC2 includes dust characterized by Ca^{2+} and
268 Mg^{2+} content; PC3 includes secondary formation characterized by SO_4^{2-} , NO_3^- , and
269 NH_4^+ content; and PC4 includes fossil fuel combustion characterized by EC. In spring,
270 PC1 includes BB (levoglucosan, mannosan, and galactosan); PC2 includes dust (Ca^{2+}
271 and Mg^{2+}) and fossil fuel combustion (EC); and PC3 includes secondary formation
272 (SO_4^{2-} , NO_3^- , and NH_4^+). The PCA results show that the chemical components of $\text{PM}_{2.5}$
273 in Ulaanbaatar were mainly affected by BB during winter and spring. Further, OC was
274 primarily influenced by BB because it correlated well with the total variance of PC1
275 during winter (0.82; Table 2) and spring (0.77; Table 3).

276

277 3.3 Relationship among BB tracers

278 The correlations among the three BB tracers levoglucosan, mannosan, and

279 galactosan are shown in Fig. 7a (winter) and 7b (spring). The correlations between
280 levoglucosan and mannosan and between levoglucosan and galactosan are strong during
281 winter ($R^2 = 0.99$ for both pairs) and spring ($R^2 = 0.95$ and 0.83 , respectively; Fig. 7a, b).
282 Concentrations of levoglucosan and OC are strongly correlated during both winter ($R^2 =$
283 0.78) and spring ($R^2 = 0.86$; Fig. 8a), suggesting that a major fraction of OC might be
284 originated from BB in Ulaanbaatar. The similar strong correlation and steep slope
285 observed in OC–levoglucosan plots for PM collected in Chiang Mai Province (Thailand)
286 and Daejeon (Korea) were attributed mainly to BB (Jung et al., 2014; Thepnuan et al.,
287 2019).

288 Fine mode K^+ is considered as biomass burning tracer in previous studies (Louie et
289 al., 2005; Deshmukh et al., 2011; Cheng et al., 2013). The moderate correlation between
290 levoglucosan and K^+ concentrations ($R^2 = 0.68$) in winter indicates that they are
291 produced from similar sources (Fig. 8b), with BB contributing most of the K^+ . However,
292 the correlation between levoglucosan and K^+ was weak in spring ($R^2 = 0.49$; Fig. 8b).
293 Because K^+ is typically emitted at a higher mass fraction in flaming phase combustion
294 compared to smoldering (Lee et al., 2010), smoldering combustion tends to have higher
295 levoglucosan/ K^+ emission ratio compared to flaming combustion (Schkolnik et al., 2005;
296 Gao et al., 2003). High levoglucosan/ K^+ ratio was observed during winter (8.92)
297 compared to spring (4.21) in this site. Thus, weak correlation between levoglucosan and
298 K^+ concentrations at Ulaanbaatar in spring can be explained by mixed burning condition
299 such as smoldering and flaming.

300 OC and K^+ concentrations correlated well during winter ($R^2 = 0.79$; Fig. 9a) and
301 spring ($R^2 = 0.73$; Fig. 9b), suggesting that they might be originated from similar
302 sources. Because most of the aerosol particles emitted from BB belong to $PM_{2.5}$, the

303 correlation between OC and K^+ as well as levoglucosan suggests that BB is one of the
304 potential sources of OC in winter and spring. Because biomass fuel is burned in
305 traditional stoves with no pollution control devices in Ulaanbaatar (Batmunkh et al.,
306 2013), soil and ash particles are entrained in convective processes and uplifted in the
307 atmosphere together with smoke particles (Deshmukh et al., 2011; Nirmalkar et al.,
308 2019).

309

310 3.4 Tracing the source of BB aerosol

311 OC is a major contributor of the quantified aerosol components in $PM_{2.5}$ in
312 Ulaanbaatar during spring and winter (Table 1). To quantify the OC_{BB} , it is necessary to
313 identify the BB fuel type. Several investigators used levoglucosan/mannosan and
314 levoglucosan/ K^+ ratios to identify BB fuel types (Puxbaum et al., 2007; Cheng et al.,
315 2013; Jung et al., 2014; Chen et al., 2018; Thepnuan et al., 2019).

316 The levoglucosan/mannosan ratio is source-specific and can be used to identify BB
317 fuel types due to the unique cellulose and hemicellulose compositions of different
318 biomass fuels (Zhang et al., 2007; Cheng et al., 2013). A previous study suggested that
319 the levoglucosan/mannosan ratio is strongly dependent on wood type, rather than on the
320 site where the wood is grown (Cheng et al., 2013). Therefore, the
321 levoglucosan/mannosan ratio was used to trace the type of wood burnt during winter
322 and spring for indoor heating and cooking purposes. Previous studies have used
323 levoglucosan/mannosan ratios to investigate the BB fuel types (Cheng et al., 2013; Jung
324 et al., 2014).

325 However, the levoglucosan/mannosan ratio can't distinguish crop residuals (29 ± 15)
326 (Sheesley et al., 2003, Sullivan et al., 2008, Engling et al., 2009, Oanh et al., 2011) and

327 hardwood (28 ± 28) (Fine et al. 2001, 2002, 2004a, b; Engling et al., 2006; Schmidl et
328 al., 2008; Bari et al., 2009; Goncalves et al., 2010) due to the overlap of ratios between
329 these fuel types (Cheng et al., 2013; Fine et al. 2001, 2002, 2004a, b; Engling et al.,
330 2006). However, levoglucosan/ K^+ ratio can distinguish between the two groups (Jung et
331 al., 2014, Chen et al., 2018). Both levoglucosan/mannosan and levoglucosan/ K^+ ratios
332 are therefore useful in distinguishing various types of fuel (Cheng et al., 2013; Puxbaum
333 et al., 2007).

334 A levoglucosan/mannosan–levoglucosan/ K^+ scatter plot based on results of the
335 present and previous studies is shown in Fig. 10, using data from Schauer et al. (2001),
336 Fine et al. (2001, 2002, 2004a, b), and Engling et al. (2006) for hardwood grown in the
337 USA; Schauer et al. (2001), Hays et al. (2002), Fine et al. (2001, 2002, 2004a, b), and
338 Engling et al. (2006) for US softwood; Schmidl et al. (2008), Bari et al. (2009) and
339 Goncalves et al. (2010) for hardwood grown in Europe; Iinuma et al. (2007), Schmidl et
340 al. (2008), and Goncalves et al. (2010) for European softwood; Engling et al. (2006) and
341 Sullivan et al. (2008) for needles and duff found in the USA; Sullivan et al. (2008) for
342 US grass; and from Sheesley et al. (2003), Sullivan et al. (2008), Engling et al. (2009)
343 and Oanh et al. (2011) for Asian rice straw.

344 The average levoglucosan/mannosan ratio was 3.6 ± 0.2 (range: 3.4 – 4.1) in winter
345 and 4.1 ± 1.0 (2.12 – 7.05) in spring, whereas the levoglucosan/ K^+ ratio was 8.9 ± 1.8
346 (5.5 – 12.4) in winter and 4.2 ± 2.1 (0.58 – 7.49) in spring at the study site (Fig. 10),
347 within the ranges reported for softwood burning sources (2.5 – 6.7 and 4.6 – 261,
348 respectively) (Fine et al., 2001; Schauer et al., 2001; Fine et al., 2002, 2004a, b; Hays et
349 al., 2002; Engling et al., 2006; Iinuma et al., 2007; Schmidl et al., 2008; Goncalves et al.,
350 2010; Cheng et al., 2013). During winter and spring, the levoglucosan/ K^+ and

351 levoglucosan/mannosan ratios in Ulaanbaatar appeared in the softwood region (Fig. 10).

352 Therefore, softwood burning seems to be the major source of BB aerosol in
353 Ulaanbaatar during both winter and spring, consistent with previously reported
354 softwood-burning emissions from fireplaces of northern and southern regions of the
355 USA (Fine et al., 2001, 2002), from household combustion in Zhengzhou, China (Chen
356 et al., 2018), and from stove wood combustion in the mid-European region (Austria;
357 Schmidl et al., 2008).

358

359 3.5 Optimization of OC/levoglucosan ratio for estimating OC_{BB} emission

360 OC_{BB} was estimated by multiplying OC/levoglucosan ratio and levoglucosan
361 concentration. Previous studies have used the OC/levoglucosan ratio obtained from
362 sources of BB aerosol to estimate OC_{BB}. A ratio of 7.35 reported for burning of four
363 types of US hardwood (Fine et al., 2002) was used for estimating OC_{BB} at four
364 background sites in Europe (Puxbaum et al., 2007). Later, mean value of 11.2 of
365 OC/levoglucosan ratio derived from ratios ranged between 4.5 – 24.6 was used for
366 estimating OC_{BB} in the UK (Harrison et al., 2012). However, such estimates may not be
367 accurate as the OC/levoglucosan ratio is highly variable in BB emissions. For example,
368 the average OC/levoglucosan ratio from softwood burning (23.8) is much higher than
369 that of hardwood burning (7.35) (Fine et al., 2002; Schmidl et al., 2008), differences are
370 more than ten-fold among studies of softwood-burning OC/levoglucosan ratios (Fine et
371 al., 2002; Hays et al., 2002; Engling et al., 2006; Iinuma et al., 2007; Goncalves et al.,
372 2010). Combustion conditions may also significantly influence OC/levoglucosan ratios.
373 For example, the OC/levoglucosan ratio varied by a factor of about seven between
374 burning the same wood (Loblolly pine) in a fireplace (27.6; Fine et al., 2002) and in a

375 stove (3.4; Fine et al., 2004b). Therefore, it is necessary to optimize the
376 OC/levoglucosan ratio for use in estimating OC_{BB}.

377 This study has used an optimized OC/levoglucosan ratio to estimate precise
378 concentration of OC_{BB} for the Ulaanbaatar study site. We have used a range of different
379 OC/levoglucosan ratios obtained from previous literatures (Fig. 11) for regression
380 analysis with measured levoglucosan concentrations to estimate optimum
381 OC/levoglucosan ratio (Fig. 12a, b). First, candidate OC_{BB} (Fig. 11) in this study was
382 estimated from OC/levoglucosan ratios for softwood burning in a previous chamber
383 experiments (Cheng et al., 2013; Schauer et al., 2001; Hays et al., 2002; Fine et al.,
384 2001, 2002, 2004a, b; Engling et al., 2006; Inuma et al., 2007; Schmidl et al., 2008;
385 Goncalves et al., 2010, Fig 11) and measured levoglucosan concentration at this site.
386 Second, OC_{non-BB} concentration was calculated by subtracting OC_{BB} from corresponding
387 total OC. If calculated OC_{non-BB} doesn't contain OC_{BB}, both regression slope and R²
388 between OC_{non-BB} versus levoglucosan will be close to zero. As shown in Fig. 12a and
389 12b, the lowest R² and regression slope were observed when OC/levoglucosan ratios of
390 27.6 and 18.0 in winter and spring, respectively. Thus, the optimized OC/levoglucosan
391 ratios for our site were determined to be 27.6 and 18.0 in winter and spring, respectively.

392 During winter higher optimum ratio of OC/levoglucosan might be due to
393 incomplete combustion during smoldering phenomena. As smoldering fires are
394 characterized by lower temperatures and thus have lower combustion efficiency, they
395 release more un-combusted condensable products, resulting in the production of more
396 unbroken organic compounds (Engling et al., 2006). Smoldering combustion generally
397 leads to increased emissions of volatile organic compounds (VOCs) and particulate
398 organic matter (OM) (Obrist et al., 2007). In contrast, the relatively lower optimum ratio

399 of OC/levoglucosan during spring might be due to the higher combustion efficiency
400 during flaming phenomena.

401 The OC_{BB} concentrations at the Ulaanbaatar study site were calculated from the
402 optimized OC/levoglucosan ratios (winter: 27.6 and spring: 18.0) and measured
403 levoglucosan concentrations. The OC_{BB} concentration was estimated to be 33.1 ± 11.9
404 $\mu\text{g C m}^{-3}$ (range 16.0–58.5 $\mu\text{g C m}^{-3}$) and $5.64 \pm 3.29 \mu\text{g C m}^{-3}$ (range 0.57–13.1 $\mu\text{g C}$
405 m^{-3}), accounting for 68% and 63% of the total OC in winter and spring, respectively
406 (Fig. 13). The average of previously published OC/levoglucosan ratios, 10.1 ± 7.9
407 (range 1.90 – 27.6), gives an estimated OC_{BB} concentration of $12.1 \pm 4.4 \mu\text{g C m}^{-3}$
408 (range 5.9–21.4 $\mu\text{g C m}^{-3}$) and $3.2 \pm 1.8 \mu\text{g C m}^{-3}$ (0.32–7.34 $\mu\text{g C m}^{-3}$) in winter and
409 spring, respectively. Their values are 2.7 (winter) and 1.8 (spring) times lower than
410 values estimated using our optimized OC/levoglucosan ratio.

411 Our estimated contribution of OC_{BB} was higher than that in Daejeon, South Korea
412 (24%–68% of total OC, mean $45\% \pm 12\%$; Jung et al., 2014) and Beijing, China (50%
413 of total OC; Cheng et al., 2013), where BB aerosols are produced mainly by the burning
414 of crop residues. The contribution of OC_{BB} to total OC is 57% and 31% during heating
415 (average temperature 0.6°C) and non-heating (average temperature 14°C) seasons in
416 Krynica Zdroj, Poland (Klejnowski et al., 2017), significantly lower than that of
417 Ulaanbaatar during both winter (average temperature -21°C) and spring (average
418 temperature 6°C). Such high concentrations of OC_{BB} in Ulaanbaatar and Krynica Zdroj
419 are likely due to intense wood burning for heating during winter.

420

421 3.6 Tracing sources of $OC_{\text{non-BB}}$

422 High concentration of $OC_{\text{non-BB}}$ was found during winter compared to spring (Fig.

423 13). Elevated $OC_{\text{non-BB}}$ could be attributed to enhanced emission from combustions and
424 favorable meteorological conditions (cold temperatures and inversion conditions, etc.)
425 during the winter. There is strong correlation between $OC_{\text{non-BB}}$ and SO_4^{2-} , NH_4^+ , and K^+
426 in winter and $OC_{\text{non-BB}}$ and NO_3^- , Na^+ , K^+ , Mg^{2+} , Ca^{2+} , and EC in spring (Table 4).
427 Residential combustion of coal emits significant amounts of OC, EC, and inorganic
428 species (SO_4^{2-} and metals) due to incomplete combustion and lack of pollution control
429 devices (Garcia et al., 1992; Li et al., 2016; Watson et al., 2001a, b). Garcia et al. (1992)
430 studied emissions of volatile organic compounds from coal burning and vehicle engines.

431 In Ulaanbaatar, the use of wood and coal for cooking and heating, and emissions
432 from old vehicles are reported as potential sources of OC (Batmunkh et al., 2013;
433 Zhamsueva et al., 2018). The three thermal power plants in Ulaanbaatar are point
434 sources for emissions of carbonaceous aerosol (Batmunkh et al., 2013), burning ~5
435 million tons of coal per year (Batmunkh et al., 2013). High concentrations of anions
436 (SO_4^{2-} and NO_3^-) and cations (NH_4^+ and Na^+) are reported in China (Zhou et al., 2003),
437 the USA (Caiazza et al., 2013), Brazil (Flues et al., 2002), India (Guttikunda and
438 Jawahar, 2014), Korea (Park and Kim, 2004; Park et al., 2015), and Spain (Alastuey et
439 al., 1999) near coal-fired thermal power plants. Emissions of volatile organic
440 compounds from vegetation have also been observed in previous studies (Fehsenfeld et
441 al., 1992; Shao et al., 2001; Acton et al., 2016). The correlations of $OC_{\text{non-BB}}$ with ions
442 and EC are thus likely due to volatile organic compounds emitted from coal-burning
443 and vehicles, and vegetative emissions.

444

445 **4. Conclusions**

446 BB was identified as a major source of the quantified aerosol components in $PM_{2.5}$

447 in Ulaanbaatar, Mongolia, during the winter and spring of 2017, based on PCA. OC was
448 the major component of the quantified aerosol components during the entire sampling
449 period, winter and spring. For determination of OC_{BB}, the fuel type must be identified
450 and levoglucosan/mannosan and levoglucosan/K⁺ ratios obtained from previous studies
451 and our on-site measurements were used for this purpose.

452 Softwood burning was identified as a major source of OC_{BB}. However,
453 OC/levoglucosan ratios from softwood burning are highly variable, and an optimum
454 ratio was derived by regression analysis between daily concentrations of OC_{non-BB} and
455 levoglucosan, yielding values of 27.6 and 18.0 for winter and spring, respectively. The
456 application of these ratios indicates that 68% and 63% of the OC originated from BB
457 during winter and spring, respectively, which is about double that estimated using
458 average values of previous studies. The atmospheric concentration of OC_{BB} was higher
459 in winter than in spring mainly due to additional BB for heating and cooking. BB
460 aerosols in Ulaanbaatar originate mainly from local softwood burning. The approach
461 developed here may be applied elsewhere for screening region-specific
462 OC/levoglucosan ratios for estimating atmospheric appropriate concentrations of OC_{BB},
463 aiding the establishment of BB control measures.

464

465 **Author contribution**

466 Jinsang Jung and Tsatsral Batmunkh designed the study and carried out the field
467 work. Jinsang Jung performed chemical analyses and quality-control measures. Jayant
468 Nirmalkar wrote the manuscript under the guidance of Jinsang Jung. All authors
469 commented on and discussed the manuscript.

470

471 **Competing interests**

472 The authors declare that they have no conflict of interests.

473

474 **Acknowledgments**

475 This work was funded by a grant (19011057) from the Korea Research Institute of
476 Standards and Science (KRISS) under the Basic R&D Project of Quantification of local
477 and long-range transported pollutants during a severe haze episode over the Korean
478 Peninsula. The authors gratefully acknowledge the NOAA Air Resources Laboratory for
479 the provision of the HYSPLIT transport and dispersion model and access to the READY
480 website (<http://www.arl.noaa.gov/ready.html>) and the Fire Information for Resource
481 Management System (FIRMS) of the National Aeronautics and Space Administration
482 (NASA), United States (<https://firms.modaps.eosdis.nasa.gov/alerts/>) used in this study.

483

484 **Data availability**

485 The data used in this study are available from the corresponding author upon
486 request (jsjung@kriss.re.kr).

487

488

489 **References**

- 490 Achad, M., Caumo, S., de Castro Vasconcellos, P., Bajano, H., Gómez, D., and
491 Smichowski, P.: Chemical markers of biomass burning: Determination of
492 levoglucosan, and potassium in size-classified atmospheric aerosols collected in
493 Buenos Aires, Argentina by different analytical techniques, *Microchem. J.*, 139,
494 181–187, <https://doi.org/10.1016/j.microc.2018.02.016>, 2018.
- 495 Acton, W. J. F., Schallhart, S., Langford, B., Valach, A., Rantala, P., Fares, S., and
496 Carriero, G.: Canopy-scale flux measurements and bottom-up emission estimates
497 of volatile organic compounds from a mixed oak and hornbeam forest in northern
498 Italy, *Atmos. Chem. Phys.*, 16, 7149–7170, [https://doi.org/10.5194/acp-16-7149-](https://doi.org/10.5194/acp-16-7149-2016)
499 2016, 2016.
- 500 Alastuey, A., Querol, X., Chaves, A., Ruiz, C. R., Carratala, A., and Lopez-Soler, A.:
501 Bulk deposition in a rural area located around a large coal-fired power station,
502 northeast Spain, *Environ. Pollut.*, 106(3), 359–367,
503 [https://doi.org/10.1016/S0269-7491\(99\)00103-7](https://doi.org/10.1016/S0269-7491(99)00103-7), 1999.
- 504 Allan, J. D., Morgan, W. T., Darbyshire, E., Flynn, M. J., Williams, P. I., Oram, D. E.,
505 Artaxo, P., Brito, J., Lee, J. D., and Coe, H.: Airborne observations of IEPOX-
506 derived isoprene SOA in the Amazon during SAMBBA, *Atmos. Chem. Phys.*, 14,
507 11393–11407, <https://doi.org/10.5194/acp-14-11393-2014>, 2014.
- 508 Ashbaugh, L.L., Malm, W.C., and Sadeh, W.Z.: A residence time probability analysis of
509 sulfur concentrations at Grand Canyon National Park, *Atmos. Environ.*, 19(8),
510 1263–1270, [https://doi.org/10.1016/0004-6981\(85\)90256-2](https://doi.org/10.1016/0004-6981(85)90256-2), 1985.
- 511 Bari, M. A., Baumbach, G., Kuch, B., and Scheffknecht, G.: Wood smoke as a source of
512 particle-phase organic compounds in residential areas, *Atmos. Environ.*, 43,
513 4722–4732, <https://doi.org/10.1016/j.atmosenv.2008.09.006>, 2009.
- 514 Batmunkh, T., Kim, Y. J., Jung, J. S., Park, K., and Tumendemberel, B.: Chemical
515 characteristics of fine particulate matters measured during severe winter haze
516 events in Ulaanbaatar, Mongolia, *J. Air & Waste Manag. Assoc.*, 63, 659–670,
517 <https://doi.org/10.1080/10962247.2013.776997>, 2013.
- 518 Caiazzo, F., Ashok, A., Waitz, I. A., Yim, S. H., and Barrett, S. R.: Air pollution and
519 early deaths in the United States. Part I: Quantifying the impact of major sectors
520 in 2005, *Atmos. Environ.*, 79, 198–208,

521 <https://doi.org/10.1016/j.atmosenv.2013.05.081>, 2013.

522 Cao, J. J., Wu, F., Chow, J. C., Lee, S. C., Li, Y., Chen, S. W., An, Z. S., Fung, K. K.,
523 Watson, J. G., Zhu, C. S., and Liu, S. X.: Characterization and source
524 apportionment of atmospheric organic and elemental carbon during fall and winter
525 of 2003 in Xi'an, China, *Atmos. Chem. Phys.*, 5, 3127–3137,
526 <https://doi.org/10.5194/acp-5-3127-2005>, 2005.

527 Chantara, S., Thepnuan, D., Wiriya, W., Prawan, S., and Tsai, Y. I.: Emissions of
528 pollutant gases, fine particulate matters and their significant tracers from biomass
529 burning in an open-system combustion chamber, *Chemosphere*, 224, 407–416,
530 2019.

531 Chen, H., Yin, S., Li, X., Wang, J., and Zhang, R.: Analyses of biomass burning
532 contribution to aerosol in Zhengzhou during wheat harvest season in 2015, *Atmos.*
533 *Res.*, 207, 62–73, <https://doi.org/10.1016/j.atmosres.2018.02.025>, 2018.

534 Cheng, Y., Engling, G., He, K.-B., Duan, F.-K., Ma, Y.-L., Du, Z.-Y., Liu, J.-M., Zheng,
535 M., and Weber, R. J.: Biomass burning contribution to Beijing aerosol, *Atmos.*
536 *Chem. Phys.*, 13, 7765–7781, <https://doi.org/10.5194/acp-13-7765-2013>, 2013.

537 Chung, S. and Chon, H. T.: Assessment of the level of mercury contamination from
538 some anthropogenic sources in Ulaanbaatar, Mongolia, *J. Geochem. Explor.*, 147,
539 237–244, <https://doi.org/10.1016/j.gexplo.2014.07.016>, 2014.

540 Claeys, M., Kourtchev, I., Pashynska, V., Vas, G., Vermeylen, R., Wang, W., Cafmeyer,
541 J., Chi, X., Artaxo, P., Andreae, M. O., and Maenhaut, W.: Polar organic marker
542 compounds in atmospheric aerosols during the LBA-SMOCC 2002 biomass
543 burning experiment in Rondônia, Brazil: sources and source processes, time series,
544 diel variations and size distributions, *Atmos. Chem. Phys.*, 10, 9319–9331,
545 <https://doi.org/10.5194/acp-10-9319-2010>, 2010.

546 Deshmukh, D. K., Deb, M. K., Tsai, Y. I., and Mkoma, S. L.: Water soluble ions in
547 PM_{2.5} and PM₁ aerosols in Durg city, Chhattisgarh, India, *Aerosol Air Qual. Res.*,
548 11, 696-708, 10.4209/aaqr.2011.03.0023, 2011.

549 Deshmukh, D. K., Haque, M. M., Kim, Y., and Kawamura, K.: Organic tracers of fine
550 aerosol particles in central Alaska: summertime composition and sources, *Atmos.*
551 *Chem. Phys.*, 19, 14009–14029, <https://doi.org/10.5194/acp-19-14009-2019>, 2019.

552 Davy, P. K., Gunchin, G., Markwitz, A., Trompeter, W. J., Barry, B. J., Shagijamba, D.,

553 and Lodoysamba, S.: Air particulate matter pollution in Ulaanbaatar, Mongolia:
554 determination of composition, source contributions and source locations, *Atmos.*
555 *Poll. Res.*, 2, 126-137, <https://doi.org/10.5094/APR.2011.017>, 2011.

556 Duan, F., Liu, X., Yu, T., and Cachier, H.: Identification and estimate of biomass
557 burning contribution to the urban aerosol organic carbon concentrations in Beijing,
558 *Atmos. Environ.* 38, 1275–1282, <https://doi.org/10.1016/j.atmosenv.2003.11.037>,
559 2004.

560 Engling, G., Carrico, C. M., Kreidenweis, S. M., Collett Jr., J. L., Day, D. E., Malm, W.
561 C., Lincoln, L., Hao, W. M., Iinuma, Y., and Herrmann, H.: Determination of
562 levoglucosan in biomass combustion aerosol by high-performance anion-
563 exchange chromatography with pulsed amperometric detection, *Atmos. Environ.*,
564 40, 299–311, <https://doi.org/10.1016/j.atmosenv.2005.12.069>, 2006.

565 Engling, G., Lee, J. J., Tsai, Y. W., Lung, S. C. C., Chou, C. C. K., and Chan, C. Y.: Size
566 resolved anhydrosugar composition in smoke aerosol from controlled field
567 burning of rice straw, *Aerosol Sci. Technol.*, 43, 662–672,
568 <https://doi.org/10.1080/0278682090282511>, 2009.

569 Fang, G. C., Chang, C. N., Chu, C. C., Wu, Y. S., Fu, P. P. C., Yang, I. L., and Chen, M.
570 H.: Characterization of particulate, metallic elements of TSP, PM_{2.5} and PM_{2.5-10}
571 aerosols at a farm sampling site in Taiwan, Taichung, *Sci. Tot. Environ.*, 308,
572 157–166, [https://doi.org/10.1016/S0048-9697\(02\)00648-4](https://doi.org/10.1016/S0048-9697(02)00648-4), 2003.

573 Fehsenfeld, F., Calvert, J., Fall, R., Goldan, P., Guenther, A. B., Hewitt, C. N., Lamb, B.,
574 Liu, S., Trainer, M., Westberg, H., and Zimmerman, P.: Emissions of volatile
575 organic compounds from vegetation and the implications for atmospheric
576 chemistry, *Global Biogeochem. Cy.*, 6, 389–430,
577 <https://doi.org/10.1029/92GB02125>, 1992.

578 Feng, Y., Chen, Y., Guo, H., Zhi, G., Xiong, S., Li, J., Sheng, G., and Fu, J.:
579 Characteristics of organic and elemental carbon in PM_{2.5} samples in Shanghai,
580 China, *Atmos. Res.*, 92, 434–442, <https://doi.org/10.1016/j.atmosres.2009.01.003>,
581 2009.

582 Fine, P. M., Cass, G. R., and Simoneit, B. R. T.: Chemical characterization of fine
583 particle emissions from fireplace combustion of woods grown in the northeastern
584 United States, *Environ. Sci. Technol.*, 35, 2665–2675,

585 <https://doi.org/10.1021/es001466k>, 2001.

586 Fine, P. M., Cass, G. R., and Simoneit, B. R. T.: Chemical characterization of fine
587 particle emissions from the fireplace combustion of woods grown in the southern
588 United States, *Environ. Sci. Technol.*, 36, 1442–1451,
589 <https://doi.org/10.1021/es0108988>, 2002.

590 Fine, P. M., Cass, G. R., and Simoneit, B. R. T.: Chemical characterization of fine
591 particle emissions from the fireplace combustion of wood types grown in the
592 midwestern and western United States, *Environ. Engin. Sci.*, 21, 387–409,
593 <https://doi.org/10.1089/109287504323067021>, 2004a.

594 Fine, P. M., Cass, G. R., and Simoneit, B. R. T.: Chemical characterization of fine
595 particle emissions from the wood stove combustion of prevalent United States tree
596 species, *Environ. Engin. Sci.*, 21, 705–721, [https://doi.org/10.1089/ees.2004,](https://doi.org/10.1089/ees.2004.21.705)
597 21.705, 2004b.

598 Flues, M., Hama, P., Lemes, M. J. L., Dantas, E. S. K., and Fornaro, A.: Evaluation of
599 the rainwater acidity of a rural region due to a coal-fired power plant in Brazil,
600 *Atmos. Environ.*, 36, 2397–2404, [https://doi.org/10.1016/S1352-2310\(01\)00563-5,](https://doi.org/10.1016/S1352-2310(01)00563-5)
601 2002.

602 Fu, P. Q., Kawamura, K., Chen, J., Li, J., Sun, Y. L., Liu, Y., Tachibana, E., Aggarwal, S.
603 G., Okuzawa, K., Tanimoto, H., and Kanaya, Y.: Diurnal variations of organic
604 molecular tracers and stable carbon isotopic composition in atmospheric aerosols
605 over Mt. Tai in the North China Plain: an influence of biomass burning, *Atmos.*
606 *Chem. Phys.*, 12, 8359–8375, doi:10.5194/acp-12-8359-2012, 2012.

607 Gao, S., Hegg D. A., Hobbs P. V., Kirchstetter T. W., Magi B. I., and Sadilek M.: Water-
608 soluble organic components in aerosols associated with savanna fires in southern
609 Africa: Identification, evolution, and distribution, *J. Geophys. Res.*, 108(D13),
610 8491, doi:10.1029/2002JD002324, 2003.

611 Garcia, J., Beyne-Masclat, S., Mouvier, G., and Masclat, P.: Emissions of volatile
612 organic compounds by coal-fired power stations. *Atmos. Environ., Part A*, 26,
613 1589–1597, [https://doi.org/10.1016/0960-1686\(92\)90059-T](https://doi.org/10.1016/0960-1686(92)90059-T), 1992.

614 Gonçalves, C., Alves, C., Evtyugina, M., Mirante, F., Pio, C., Caseiro, A., Schmidl, C.,
615 Bauer, H., and Carvalho, F.: Characterisation of PM₁₀ emissions from wood stove
616 combustion of common woods grown in Portugal, *Atmos. Environ.*, 44,

617 4474–4480, <https://doi.org/10.1016/j.atmosenv.2010.07.026>, 2010.

618 Gu, J., Bai, Z., Li, W., Wu, L., Liu, A., Dong, H., and Xie, Y.: Chemical composition of
619 PM_{2.5} during winter in Tianjin, China, *Particuology*, 9, 215–221,
620 <https://doi.org/10.1016/j.partic.2011.03.001>, 2011.

621 Guttikunda, S.: Urban air pollution analysis for Ulaanbaatar, Mongolia, SIM Working
622 Paper No. 2008-005, <http://dx.doi.org/10.2139/ssrn.1288328>, 2008.

623 Guttikunda, S. K. and Jawahar, P.: Atmospheric emissions and pollution from the
624 coal-fired thermal power plants in India, *Atmos. Environ.*, 92, 449–460,
625 <https://doi.org/10.1016/j.atmosenv.2014.04.057>, 2014.

626 Harrison, R. M., Beddows, D. C. S., Hu, L., and Yin, J.: Comparison of methods for
627 evaluation of wood smoke and estimation of UK ambient concentrations, *Atmos.*
628 *Chem. Phys.*, 12, 8271–8283, doi:10.5194/acp-12-8271-2012, 2012.

629 Hays, M. D., Geron, C. D., Linna, K. J., Smith, N. D., and Schauer, J. J.: Speciation of
630 gasphase and fine particle emissions from burning of foliar fuels, *Environ. Sci.*
631 *Technol.*, 36, 2281–2295, <https://doi.org/10.1021/es0111683>, 2002.

632 Haque, M., Kawamura, K., Deshmukh, D. K., Fang, C., Song, W., Mengying, B., and
633 Zhang, Y. L.: Characterization of organic aerosols from a Chinese megacity
634 during winter: predominance of fossil fuel combustion. *Atmos. Chem. Phys.*, 19,
635 5147-5164, <https://doi.org/10.5194/acp-19-5147-2019>, 2019.

636 Huang, X., Liu, Z., Zhang, J., Wen, T., Ji, D., and Wang, Y.: Seasonal variation and
637 secondary formation of size-segregated aerosol water-soluble inorganic ions
638 during pollution episodes in Beijing, *Atmos. Res.*, 168, 70–79,
639 <https://doi.org/10.1016/j.atmosres.2015.08.021>, 2016.

640 Iinuma, Y., Brüggemann, E., Gnauk, T., Müller, K., Andreae, M. O., Helas, G., Parmar,
641 R., and Herrmann, H.: Source characterization of biomass burning particles: the
642 combustion of selected European conifers, African hardwood, savanna grass, and
643 German and Indonesian peat, *J. Geophys. Res.*, 112, D08209.
644 <http://dx.doi.org/10.1029/2006JD007120>, 2007.

645 Ji, D., Zhang, J., He, J., Wang, X., Pang, B., Liu, Z., Wang, L., and Wang, Y.:
646 Characteristics of atmospheric organic and elemental carbon aerosols in urban
647 Beijing, China, *Atmos. Environ.*, 125, 293–306,
648 <https://doi.org/10.1016/j.atmosenv.2015.11.020>, 2016.

649 Jimenez, J. L., Canagaratna, M. R., Donahue, N. M., Prevot, A. S. H., Zhang, Q., Kroll,
650 J. H., DeCarlo, P. F., Allan, J. D., Coe, H., Ng, N. L., and Aiken, A. C.: Evolution
651 of organic aerosols in the atmosphere, *Science*, 326, 1525–1529,
652 doi:10.1126/science.1180353, 2009.

653 Jung, J., Lee, H., Kim, Y. J., Liu, X., Zhang, Y., Hu, M., and Sugimoto, N.: Optical
654 properties of atmospheric aerosols obtained by in situ and remote measurements
655 during 2006 Campaign of Air Quality Research in Beijing (CAREBeijing-2006), *J.*
656 *Geophys. Res.*, 114, D00G02, doi:10.1029/2008JD010337, 2009.

657 Jung, J., Tsatsral, B., Kim, Y. J., and Kawamura, K.: Organic and inorganic aerosol
658 compositions in Ulaanbaatar, Mongolia, during the cold winter of 2007 to 2008:
659 dicarboxylic acids, ketocarboxylic acids, and α -dicarbonyls, *J. Geophys. Res.:*
660 *Atmos.*, 115, D22203, <https://doi.org/10.1029/2010JD014339>, 2010.

661 Jung, J., Lee, S., Kim, H., Kim, D., Lee, H., and Oh, S.: Quantitative determination of
662 the biomass-burning contribution to atmospheric carbonaceous aerosols in
663 Daejeon, Korea, during the rice-harvest period, *Atmos. Environ.*, 89, 642–650,
664 <https://doi.org/10.1016/j.atmosenv.2014.03.010>, 2014.

665 Khan, M. F., Shirasuna, Y., Hirano, K., and Masunaga, S.: Characterization of PM_{2.5},
666 PM_{2.5-10} and PM_{>10} in ambient air, Yokohama, Japan, *Atmos. Res.*, 96, 159-172,
667 <https://doi.org/10.1016/j.atmosres.2009.12.009>, 2010.

668 Klejnowski, K., Janoszka, K., and Czaplicka, M.: Characterization and seasonal
669 variations of organic and elemental carbon and levoglucosan in PM₁₀ in Krynica
670 Zdroj, Poland, *Atmosphere*, 8, 190, doi:10.3390/atmos8100190, 2017.

671 Lai, C., Liu, Y., Ma, J., Ma, Q., and He, H.: Degradation kinetics of levoglucosan
672 initiated by hydroxyl radical under different environmental conditions, *Atmos.*
673 *Environ.*, 91, 32–39, <https://doi.org/10.1016/j.atmosenv.2014.03.054>, 2014.

674 Lee, T., Sullivan, A. P., Mack, L., Jimenez, J. L., Kreidenweis, S. M., Onasch, T. B.,
675 Worsnop, D. R., Malm, W., Wold, C. E., Hao, W. M., and Collett Jr, J. L.:
676 Chemical smoke marker emissions during flaming and smoldering phases of
677 laboratory open burning of wildland fuels, *Aerosol Sci. Technol.*, 44, i-v,
678 <https://doi.org/10.1080/02786826.2010.499884>, 2010.

679 Li, Q., Jiang, J., Zhang, Q., Zhou, W., Cai, S., Duan, L., Ge, S., and Hao, J.: Influences
680 of coal size, volatile matter content, and additive on primary particulate matter

681 emissions from household stove combustion. *Fuel*, 182, 780-787,
682 <https://doi.org/10.1016/j.fuel.2016.06.059>, 2016.

683 Liang, L., Engling, G., Du, Z., Cheng, Y., Duan, F., Liu, X., and He, K.: Seasonal
684 variations and source estimation of saccharides in atmospheric particulate matter
685 in Beijing, China, *Chemosphere*, 150, 365–377,
686 <https://doi.org/10.1016/j.chemosphere.2016.02.002>, 2016.

687 Lin, Y.-C., Hsu, S.-C., Lin, C.-Y., Lin, S.-H., Huang, Y.-T., Chang, Y., and Zhang, Y.-L.:
688 Enhancements of airborne particulate arsenic over the subtropical free troposphere:
689 impact of southern Asian biomass burning, *Atmos. Chem. Phys.*, 18, 13865-13879,
690 <https://doi.org/10.5194/acp-18-13865-2018>, 2018.

691 Louie, P. K., Watson, J. G., Chow, J. C., Chen, A., Sin, D. W., and Lau, A. K.: Seasonal
692 characteristics and regional transport of PM_{2.5} in Hong Kong, *Atmos. Environ.*, 39,
693 1695–1710, <https://doi.org/10.1016/j.atmosenv.2004.11.017>, 2005.

694 Maenhaut, W., Nava, S., Lucarelli, F., Wang, W., Chi, X., and Kulmala, M.: Chemical
695 composition, impact from biomass burning, and mass closure for PM_{2.5} and PM₁₀
696 aerosols at Hyytiälä, Finland, in summer 2007, *X-Ray Spectrom.*, 40, 168–171,
697 <https://doi.org/10.1002/xrs.1302>, 2011.

698 Nirmalkar, J., Deshmukh, D. K., Deb, M. K., Tsai, Y. I., and Sopajaree, K.: Mass
699 loading and episodic variation of molecular markers in PM_{2.5} aerosols over a rural
700 area in eastern central India, *Atmos. Environ.*, 117, 41–50,
701 <https://doi.org/10.1016/j.atmosenv.2015.07.003>, 2015.

702 Nirmalkar, J., Deshmukh, D. K., Deb, M. K., Tsai, Y. I., and Pervez, S.: Characteristics
703 of aerosol during major biomass burning events over eastern central India in
704 winter: A tracer-based approach, *Atmos. Pollut. Res.*, 10, 817–826,
705 <https://doi.org/10.1016/j.apr.2018.12.010>, 2019.

706 Oanh, N. T. K., Ly, B. T., Tipayarom, D., Manandhar, B. R., Prapat, P., Simpson, C.D.,
707 and Liu, L.J.S.: Characterization of particulate matter emission from open burning
708 of rice straw, *Atmos. Environ.*, 45, 493–502,
709 <https://doi.org/10.1016/j.atmosenv.2010.09.023>, 2011.

710 Obrist, D., Moosmüller, H., Schürmann, R., Chen, L. W. A., and Kreidenweis, S. M.:
711 Particulate-phase and gaseous elemental mercury emissions during biomass
712 combustion: controlling factors and correlation with particulate matter emissions.

713 Environ. Sci. Technol., 42, 721-727, <https://doi.org/10.1021/es071279n>, 2007.

714 Panda, S., Sharma, S. K., Mahapatra, P. S., Panda, U., Rath, S., Mahapatra, M., Mandal,
715 T. K., and Das, T.: Organic and elemental carbon variation in PM_{2.5} over megacity
716 Delhi and Bhubaneswar, a semi-urban coastal site in India, *Nat. Hazards*, 80,
717 1709–1728, <https://doi.org/10.1007/s11069-015-2049-3>, 2016.

718 Park, S. S. and Kim, Y. J.: PM_{2.5} particles and size-segregated ionic species measured
719 during fall season in three urban sites in Korea, *Atmos. Environ.*, 38, 1459–1471,
720 <https://doi.org/10.1016/j.atmosenv.2003.12.004>, 2004.

721 Park, S. M., Seo, B. K., Lee, G., Kahng, S. H., and Jang, Y.: Chemical composition of
722 water-soluble inorganic species in precipitation at Shihwa Basin, Korea,
723 *Atmosphere*, 6, 732–750, <https://doi.org/10.3390/atmos6060732>, 2015.

724 Pei, B., Wang, X., Zhang, Y., Hu, M., Sun, Y., Deng, J., Dong, L., Fu, Q., and Yan N.:
725 Emissions and source profiles of PM_{2.5} for coal-fired boilers in the Shanghai
726 megacity, China, *Atmos. Pollut. Res.* 7, 577-584,
727 <https://doi.org/10.1016/j.apr.2016.01.005>, 2016.

728 Pio, C. A., Legrand, M., Alves, C. A., Oliveira, T., Afonso, J., Caseiro, A., Puxbaum, H.,
729 Sanchez-Ochoa, A., and Gelencser, A.: Chemical composition of atmospheric
730 aerosols during the 2003 summer intense forest fire period, *Atmos. Environ.*, 42,
731 7530–7543, <https://doi.org/10.1016/j.atmosenv.2008.05.032>, 2008.

732 Puxbaum, H., Caseiro, A., Sánchez-Ochoa, A., Kasper-Giebl, A., Claeys, M., Gelencser,
733 A., Legrand, M., Preunkert, S., and Pio, C.: Levoglucosan levels at background
734 sites in Europe for assessing the impact of biomass combustion on the European
735 aerosol background, *J. Geophys. Res.: Atmos.*, 112, D23S05,
736 <https://doi.org/10.1029/2006JD008114>, 2007.

737 Reche, C., Viana, M., Amato, F., Alastuey, A., Moreno, T., Hillamo, R., Teinila, K.,
738 Saarnio, K., Seco, R., Penuelas, J., and Mohr, C.: Biomass burning contributions
739 to urban aerosols in a coastal Mediterranean City, *Sci. Tot. Environ.*, 427,
740 175–190, <https://doi.org/10.1016/j.scitotenv.2012.04.012>, 2012.

741 Schauer, J.J., Kleeman, M.J., Cass, G.R., and Simoneit, B. R. T.: Measurement of
742 emissions from air pollution sources. 3. C1-C29 organic compounds from
743 fireplace combustion of wood, *Environ. Sci. Technol.*, 35, 1716–1728,
744 <https://doi.org/10.1021/es001331e>, 2001.

745 Schkolnik, G., Falkovich, A. H., Rudich, Y., Maenhaut, W., and Artaxo, P.: New
746 analytical method for the determination of levoglucosan, polyhydroxy compounds,
747 and 2-methylerythritol and its application to smoke and rainwater samples,
748 *Environ. Sci. Technol.* 39, 2744–2752, <https://doi.org/10.1021/es048363c>, 2005.

749 Schmidl, C., Marr, I. L., Caseiro, A., Kotianová, P., Berner, A., Bauer, H., Kasper-Giebl,
750 A., and Puxbaum, H.: Chemical characterisation of fine particle emissions from
751 wood stove combustion of common woods growing in mid-European Alpine
752 regions, *Atmos. Environ.*, 42, 126–141,
753 <https://doi.org/10.1016/j.atmosenv.2007.09.028>, 2008.

754 Shao, M., Czapiewski, K. V., Heiden, A. C., Kobel, K., Komenda, M., Koppmann, R.,
755 and Wildt, J.: Volatile organic compound emissions from Scots pine: mechanisms
756 and description by algorithms, *J. Geophys. Res.: Atmos.*, 106(D17), 20483–20491,
757 [10.1029/2000JD000248](https://doi.org/10.1029/2000JD000248), 2001.

758 Sharma, A., Pareek, V., and Zhang, D.: Biomass pyrolysis—A review of modelling,
759 process parameters and catalytic studies. *J. Renew. Sustain. Energy*, 50,
760 1081–1096, <https://doi.org/10.1016/j.rser.2015.04.193>, 2015.

761 Sheesley, R. J., Schauer, J. J., Chowdhury, Z., Cass, G. R., and Simoneit, B. R. T.:
762 Characterization of organic aerosols emitted from the combustion of biomass
763 indigenous to South Asia, *J. Geophys. Res.*, 108, 4285, [http://](http://dx.doi.org/10.1029/2002JD002981)
764 dx.doi.org/10.1029/2002JD002981, 2003.

765 Simoneit, B. R., Schauer, J. J., Nolte, C. G., Oros, D. R., Elias, V. O., Fraser, M. P.,
766 Rogge, W. F., and Cass, G. R., 1999. Levoglucosan, a tracer for cellulose in
767 biomass burning and atmospheric particles, *Atmos. Environ.*, 33, 173–182,
768 [https://doi.org/10.1016/S1352-2310\(98\)00145-9](https://doi.org/10.1016/S1352-2310(98)00145-9), 1999.

769 Sullivan, A. P., Holden, A. S., Patterson, L. A., McMeeking, G. R., Kreidenweis, S. M.,
770 Malm, W. C., Hao, W. M., Wold, C. E., and Collett Jr., J. L.: A method for smoke
771 marker measurements and its potential application for determining the
772 contribution of biomass burning from wildfires and prescribed fires to ambient
773 PM_{2.5} organic carbon, *J. Geophys. Res.*, 113, D22302, [http://](http://dx.doi.org/10.1029/2008JD010216)
774 dx.doi.org/10.1029/2008JD010216, 2008.

775 Sullivan, A. P., Guo, H., Schroder, J. C., Campuzano-Jost, P., Jimenez, J. L., Campos, T.,
776 Shah, V., Jaegle, L., Lee, B. H., Lopez-Hilfiker, F. D., and Thornton, J. A.:

777 Biomass burning markers and residential burning in the winter aircraft campaign.
778 *J. Geophys. Res.: Atmos.*, 124, 1846–1861,
779 <https://doi.org/10.1029/2017JD028153>, 2019.

780 Sun, J., Shen, Z., Zhang, Y., Zhang, Q., Wang, F., Wang, T., Chang, X., Lei, Y., Xu, H.,
781 Cao, J., and Zhang, N.: Effects of biomass briquetting and carbonization on
782 PM_{2.5} emission from residential burning in Guanzhong Plain, China, *Fuel*, 244,
783 379–387, <https://doi.org/10.1016/j.fuel.2019.02.031>, 2019.

784 Tao, J., Zhang, L., Ho, K., Zhang, R., Lin, Z., Zhang, Z., Lin, M., Cao, J., Liu, S., and
785 Wang, G.: Impact of PM_{2.5} chemical compositions on aerosol light scattering in
786 Guangzhou—the largest megacity in South China, *Atmos. Res.*, 135, 48–58,
787 <https://doi.org/10.1016/j.atmosres.2013.08.015>, 2014.

788 Thepnuan, D., Chantara, S., Lee, C. T., Lin, N. H., and Tsai, Y. I.: Molecular markers for
789 biomass burning associated with the characterization of PM_{2.5} and component
790 sources during dry season haze episodes in Upper South East Asia, *Sci. Tot.*
791 *Environ.*, 658, 708–722, <https://doi.org/10.1016/j.scitotenv.2018.12.201>, 2019.

792 Verma, V., Fang, T., Guo, H., King, L., Bates, J. T., Peltier, R. E., Edgerton, E., Russell,
793 A. G., and Weber, R. J.: Reactive oxygen species associated with water-soluble
794 PM_{2.5} in the southeastern United States: spatiotemporal trends and source
795 apportionment, *Atmos. Chem. Phys.*, 14, 12915–12930,
796 <https://doi.org/10.5194/acp-14-12915-2014>, 2014.

797 Wang, T., Tian, M., Ding, N., Yan, X., Chen, S. J., Mo, Y. Z., Yang, W. Q., Bi, X. H.,
798 Wang, X. M., and Mai, B. X.: Semivolatile organic compounds (SOCs) in fine
799 particulate matter (PM_{2.5}) during clear, fog, and haze episodes in winter in Beijing,
800 China, *Environ. Sci. Tech.*, 52, 5199–5207,
801 <https://doi.org/10.1021/acs.est.7b06650>, 2018.

802 Watson, J. G., Chow, J. C., and Fujita, E. M.: Review of volatile organic compound
803 source apportionment by chemical mass balance, *Atmos. Environ.*, 35, 1567–1584,
804 [https://doi.org/10.1016/S1352-2310\(00\)00461-1](https://doi.org/10.1016/S1352-2310(00)00461-1), 2001a.

805 Watson, J. G., Chow, J. C., and Houck, J. E.: PM_{2.5} chemical source profiles for vehicle
806 exhaust, vegetative burning, geological material, and coal burning in
807 Northwestern Colorado during 1995, *Chemosphere*, 43, 1141–1151,
808 [https://doi.org/10.1016/S0045-6535\(00\)00171-5](https://doi.org/10.1016/S0045-6535(00)00171-5), 2001b.

809 Zhamsueva, G. S., Zayakhanov, A. S., Starikov, A. V., Balzhanov, T. S., Tsydyпов, V. V.,
810 Demytyeva, A. L., and Khodzher, T. V.: Investigation of chemical composition of
811 atmospheric aerosol in Ulaanbaatar during 2005–2014. *Geography and Natural* 39,
812 270–276, [10.1134/S1875372818030113](https://doi.org/10.1134/S1875372818030113), 2018

813 Zhang, F., Wang, Z. W., Cheng, H. R., Lv, X. P., Gong, W., Wang, X. M., and Zhang, G.:
814 Seasonal variations and chemical characteristics of PM_{2.5} in Wuhan, central China,
815 *Sci. Tot. Environ.*, 518, 97–105, <https://doi.org/10.1016/j.scitotenv.2015.02.054>,
816 2015.

817 Zhang, Y. X., Min, S., Zhang, Y. H., Zeng, L. M., He, L. Y., Bin, Z. H. U., Wei, Y. J.,
818 and Zhu, X. L.: Source profiles of particulate organic matters emitted from cereal
819 straw burnings. *J. Environ. Sci.*, 19, 167–175, [https://doi.org/10.1016/S1001-](https://doi.org/10.1016/S1001-0742(07)60027-8)
820 [0742\(07\)60027-8](https://doi.org/10.1016/S1001-0742(07)60027-8), 2007.

821 Zhou, Y., Levy, J. I., Hammitt, J. K., and Evans, J. S.: Estimating population exposure to
822 power plant emissions using CALPUFF: a case study in Beijing, China, *Atmos.*
823 *Environ.*, 37, 815–826, [https://doi.org/10.1016/S1352-2310\(02\)00937-8](https://doi.org/10.1016/S1352-2310(02)00937-8), 2003.

824 Zhu, C., Kawamura, K., and Kunwar, B.: Effect of biomass burning over the western
825 North Pacific Rim: wintertime maxima of anhydrosugars in ambient aerosols from
826 Okinawa, *Atmos. Chem. Phys.*, 15, 1959–1973, [https://doi.org/10.5194/acp-15-](https://doi.org/10.5194/acp-15-1959-2015)
827 [1959-2015](https://doi.org/10.5194/acp-15-1959-2015), 2015.

828

829

830

831
832
833
834
835
836
837
838
839

Table 1. Concentrations ($\mu\text{g m}^{-3}$) of organic carbon, elemental carbon, levoglucosan, mannosan, galactosan, and water-soluble ions in $\text{PM}_{2.5}$ samples collected from Ulaanbaatar, Mongolia, during the winter (n = 17) and spring (n = 17) of 2017.

	OC	EC	Levoglucosan	Mannosan	Galactosan	Cl ⁻	SO ₄ ²⁻	NO ₃ ⁻	Na ⁺	NH ₄ ⁺	K ⁺	Mg ²⁺	Ca ²⁺	Temperature (°C)	Wind Speed (m sec ⁻¹)	RH (%)
Winter																
Mean	49.06	1.71	1.20	0.33	0.24	1.69	9.74	4.17	0.64	6.18	0.13	0.05	0.60	-20.8	1.36	66.1
SD	17.32	0.58	0.43	0.13	0.09	0.76	3.37	1.69	0.44	2.42	0.04	0.02	0.24	4.74	0.73	4.56
Min	24.62	0.79	0.58	0.15	0.10	0.26	2.17	0.76	0.10	3.16	0.08	0.02	0.22	-27.8	0.41	58.5
Max	79.07	3.34	2.12	0.61	0.43	2.89	16.06	7.51	1.34	11.59	0.18	0.08	1.04	-10.5	3.55	72.7
Spring																
Mean	8.50	1.11	0.31	0.08	0.04	0.30	1.90	0.70	0.13	0.74	0.08	0.04	0.93	6.11	2.60	35.1
SD	3.55	0.42	0.18	0.04	0.02	0.11	0.50	0.32	0.04	0.28	0.05	0.02	0.36	6.16	0.79	13.9
Min	2.80	0.60	0.03	0.01	0.00	0.11	1.04	0.10	0.07	0.33	0.02	0.02	0.48	-1.52	1.64	17.8
Max	16.63	2.03	0.73	0.15	0.08	0.51	3.02	1.40	0.21	1.47	0.22	0.08	1.61	15.9	4.56	65.2

840

841 Table 2. Source identification of chemical species using principal component (PC) analysis and varimax rotation at Ulaanbaatar,
 842 Mongolia, during winter of 2017.

Winter Chemical species	Component			
	PC1 (Biomass Burning)	PC2 (Dust)	PC3 (Secondary formation)	PC4 (Fossil fuel combustion)
Levoglucosan	0.96	-0.06	0.24	0.06
Mannosan	0.95	-0.08	0.27	0.06
Galactosan	0.95	-0.07	0.28	0.04
Cl ⁻	0.19	0.94	-0.05	-0.07
SO ₄ ²⁻	0.43	0.01	0.88	0.09
NO ₃ ⁻	0.28	0.20	0.87	0.20
Na ⁺	-0.27	0.87	-0.33	-0.17
NH ₄ ⁺	0.48	-0.12	0.86	0.07
K ⁺	0.70	0.11	0.61	0.25
Mg ₂ ⁺	-0.15	0.90	0.25	0.26
Ca ₂ ⁺	-0.12	0.92	0.19	0.24
OC	0.82	-0.17	0.47	0.07
EC	0.14	0.14	0.19	0.95
Eigenvalues	4.54	3.44	3.30	1.20
% of Variance	34.95	26.49	25.37	9.21
Cumulative %	34.95	61.44	86.81	96.02

843

844

845 Table 3. Source identification of chemical species using PCA and varimax rotation at Ulaanbaatar, Mongolia, during spring of 2017.

Spring	Component		
	PC1 (Biomass Burning)	PC2 (Dust and Fossil fuel combustion)	PC3 (Secondary formation)
Levoglucosan	0.88	0.13	0.39
Mannosan	0.94	0.00	0.30
Galactosan	0.95	-0.11	0.20
Cl ⁻	0.81	0.32	-0.03
SO ₄ ²⁻	0.18	0.12	0.93
NO ₃ ⁻	0.59	0.54	0.52
Na ⁺	0.08	0.91	-0.09
NH ₄ ⁺	0.44	0.05	0.88
K ⁺	0.41	0.67	0.55
Mg ²⁺	0.05	0.90	0.35
Ca ²⁺	0.10	0.97	0.15
OC	0.77	0.41	0.46
EC	0.10	0.94	0.01
Eigenvalues	4.59	4.53	2.87
% of Variance	35.30	34.84	22.04
Cumulative %	35.30	70.14	92.18

846

Table 4. Correlation coefficients (r) from Spearman correlation analysis for OC_{non-BB} and water-soluble ions during winter and spring of 2017 at Ulaanbaatar, Mongolia.

		Cl ⁻	SO ₄ ²⁻	NO ₃ ⁻	Na ⁺	NH ₄ ⁺	K ⁺	Mg ²⁺	Ca ²⁺	EC
OC _{non-BB}	Winter	-0.26	0.71**	0.44	-0.58*	0.72**	0.64**	-0.16	-0.16	0.15
	Spring	0.29	0.37	0.59*	0.74**	0.23	0.65**	0.78**	0.77**	0.74**

*Correlation is significant at the .05 level (2-tailed); **Correlation is significant at the .01 level (2-tailed).

848

849 **Figure captions**

850 Fig. 1 Sampling site in Ulaanbataar, Mongolia (<https://www.google.com/earth/versions/#earth-pro>, © Google Earth).

851 Fig. 2 Daily variations in atmospheric concentrations ($\mu\text{g m}^{-3}$) of chemical species in Ulaanbaatar during winter (a) and spring (b) of
852 2017.

853 Fig. 3 Daily atmospheric concentrations of OC ($\mu\text{g C m}^{-3}$) as a function of wind speed (m s^{-1}) and temperature ($^{\circ}\text{C}$) during winter (a)
854 and spring (b) of 2017.

855 Fig. 4 Relationship between $\text{PM}_{2.5}$ concentrations of Ca^{2+} and EC ($\mu\text{g m}^{-3}$) during spring of 2017.

856 Fig. 5 Conditional Probability Function (CPF) of levoglucosan (levo), OC, K^{+} , EC, Ca^{2+} during winter (a) and spring (b) of 2017.

857 Fig. 6 (a) Five-day backward air-mass trajectories (<https://ready.arl.noaa.gov/HYSPLIT.php>) and (b) FIRMS fire counts
858 (<https://firms.modaps.eosdis.nasa.gov/alerts/>) around Ulaanbaatar during spring of 2017.

859 Fig. 7 Correlations of $\text{PM}_{2.5}$ concentrations ($\mu\text{g m}^{-3}$) of mannosan and galactosan with levoglucosan during winter (a) and spring (b) of
860 2017.

861 Fig. 8 Correlation between $\text{PM}_{2.5}$ concentrations of (a) OC ($\mu\text{g C m}^{-3}$) and levoglucosan ($\mu\text{g m}^{-3}$) and (b) K^{+} and levoglucosan ($\mu\text{g m}^{-3}$)
862 during winter and spring of 2017.

863 Fig. 9 Correlation between $\text{PM}_{2.5}$ concentrations of OC ($\mu\text{g C m}^{-3}$) and K^{+} ($\mu\text{g m}^{-3}$) during winter (a) and spring (b) of 2017.

864 Fig. 10 Scatter plot of levoglucosan/ K^+ versus levoglucosan/mannosan from different types of BB emissions, including those measured
865 in Ulaanbaatar (blue circles and red squares).

866 Fig. 11 Comparison of previously reported OC/levoglucosan ratios for softwood burning.

867 Fig. 12 Graphical determination of optimized OC/levoglucosan ratios used to estimate $PM_{2.5}$ concentrations of OC_{BB} in Ulaanbaatar in
868 winter (a) and spring (b) of 2017.

869 Fig. 13 Relative contributions ($\mu g C m^{-3}$) of OC_{BB} and OC_{non-BB} to $PM_{2.5}$ in Ulaanbaatar during winter and spring of 2017.

870

871

872

873

874

875

876

877

878

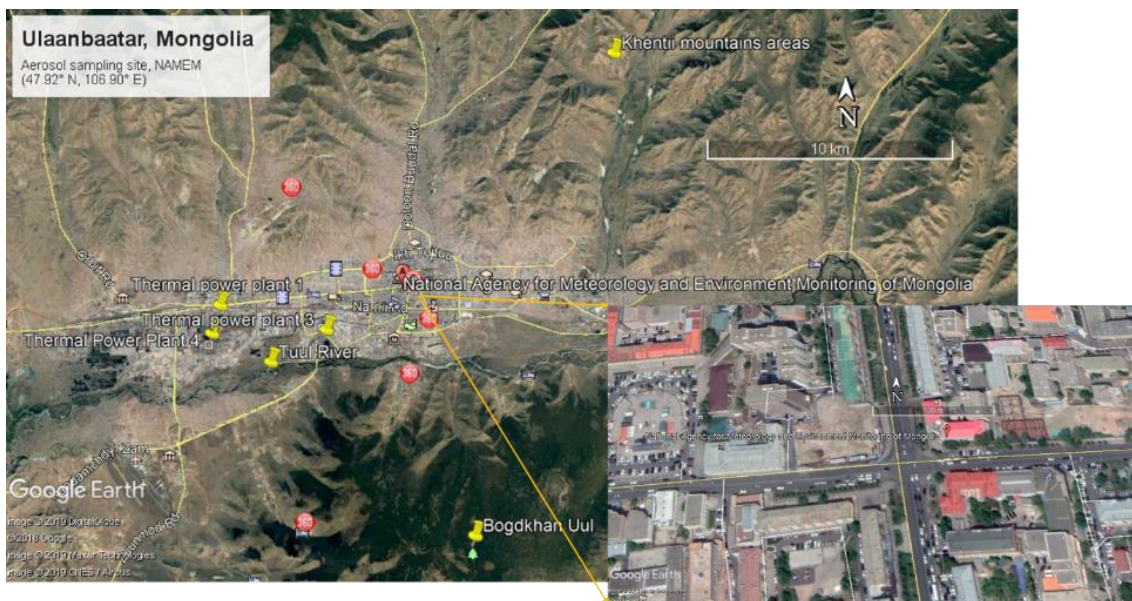
879

880

881

882

Fig. 1

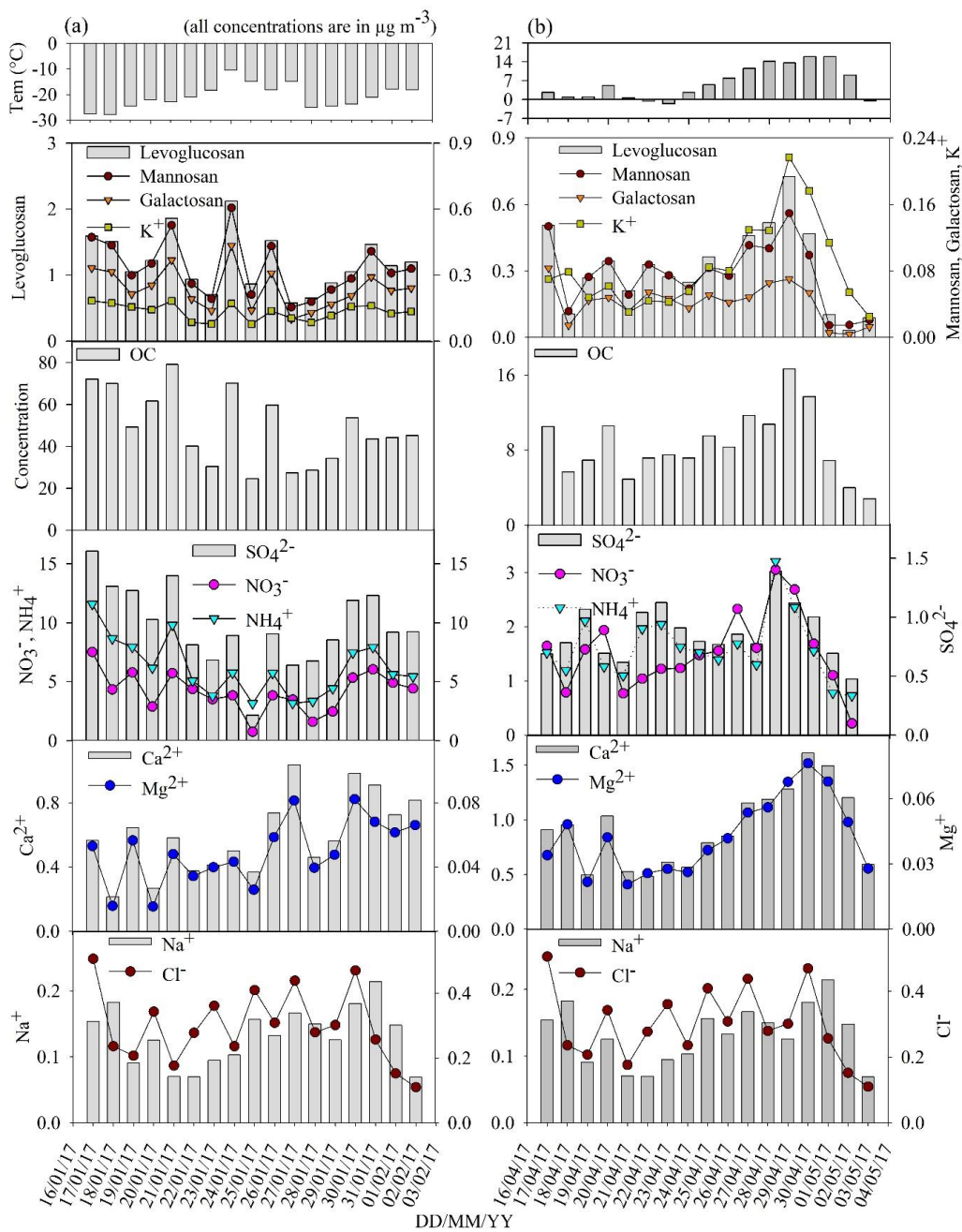


883

884

885
886

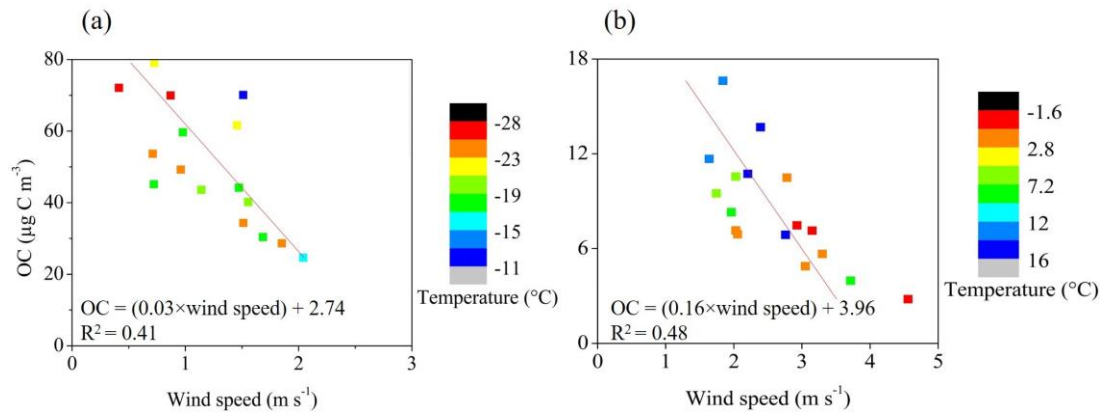
Fig. 2



887

888
889
890
891
892

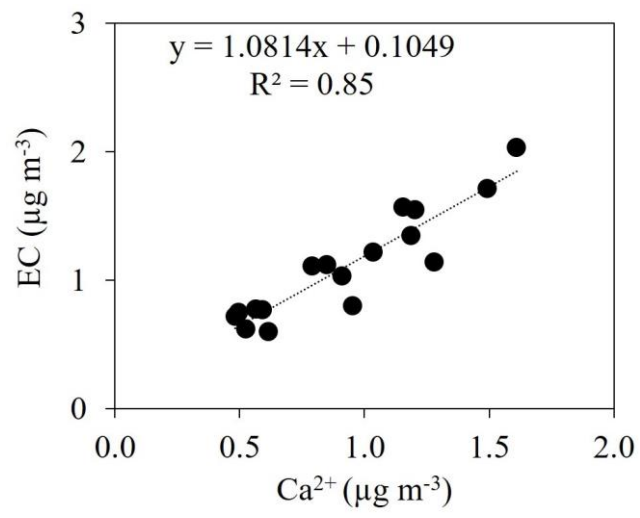
Fig. 3



893
894
895

896
897
898

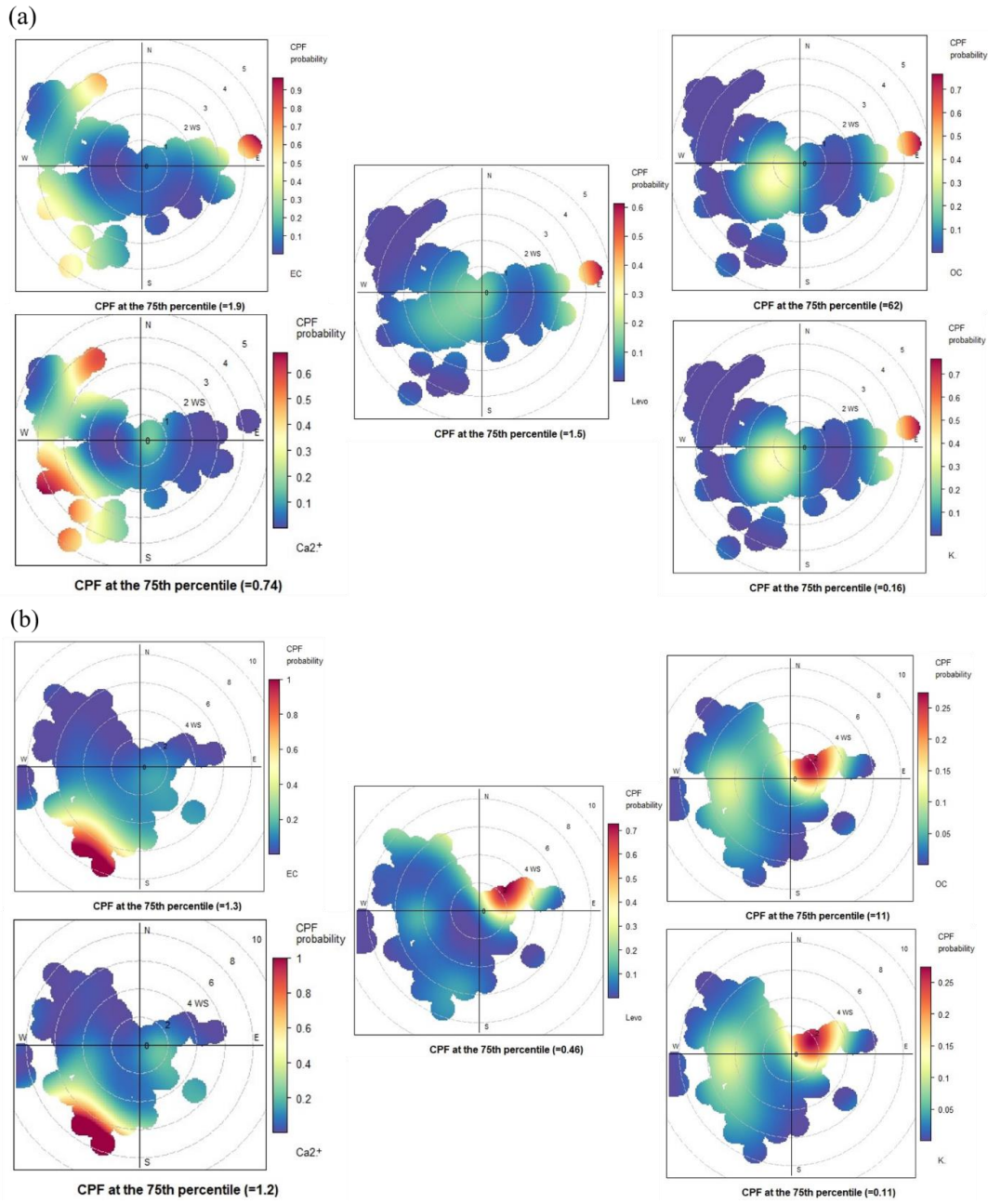
Fig. 4



899
900
901

902
903

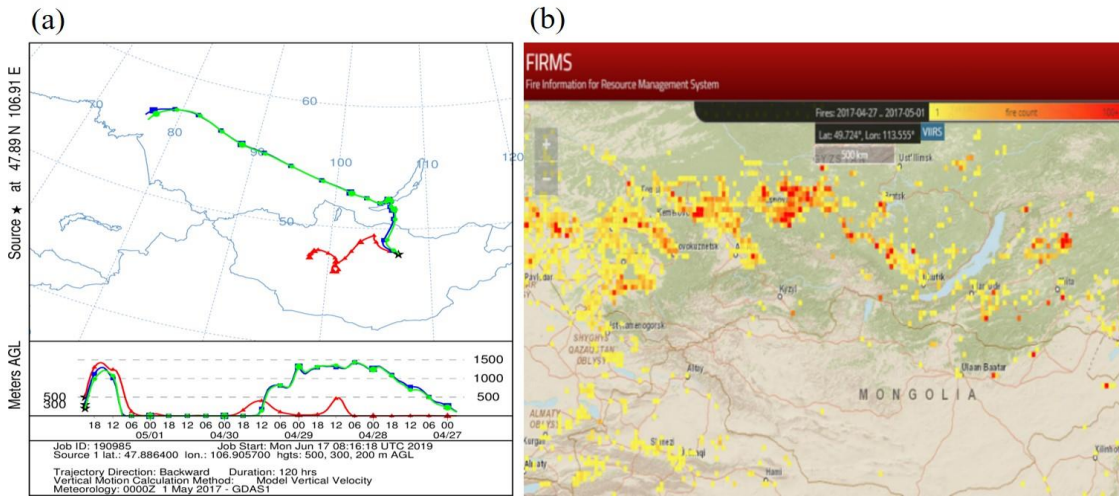
Fig. 5



904
905
906
907
908
909
910
911

912
913

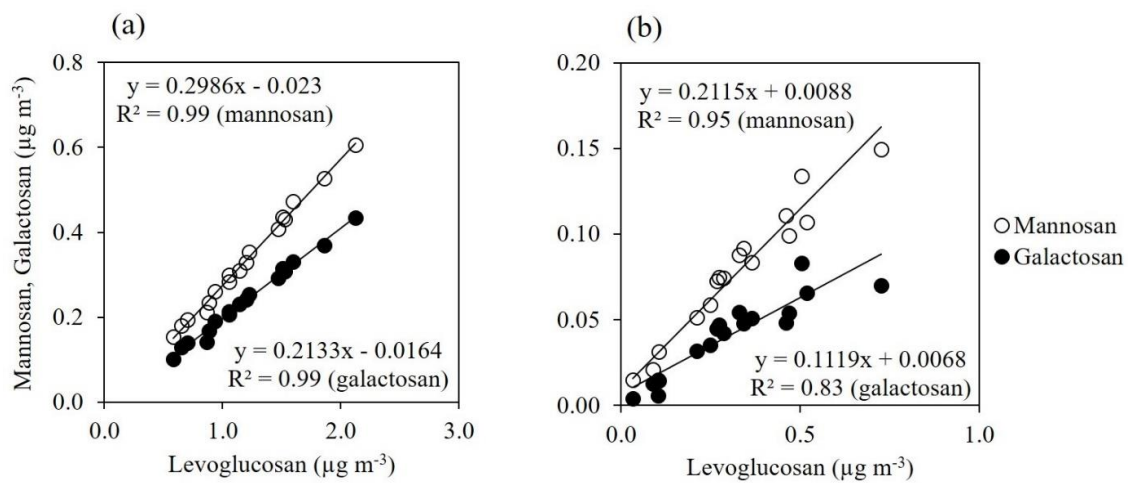
Fig. 6



914
915
916

917
918

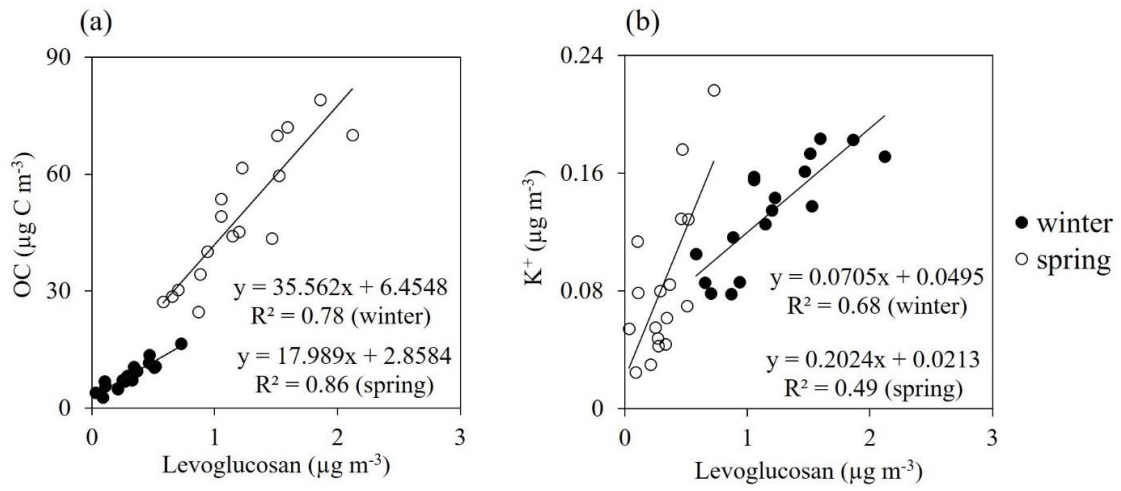
Fig. 7



919
920

921
922

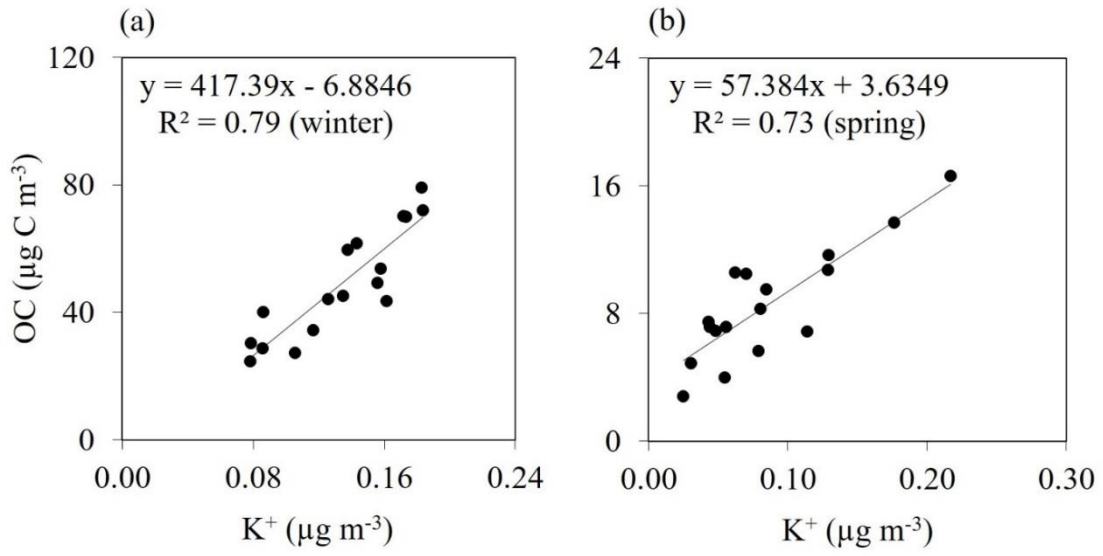
Fig. 8



923
924

925
926

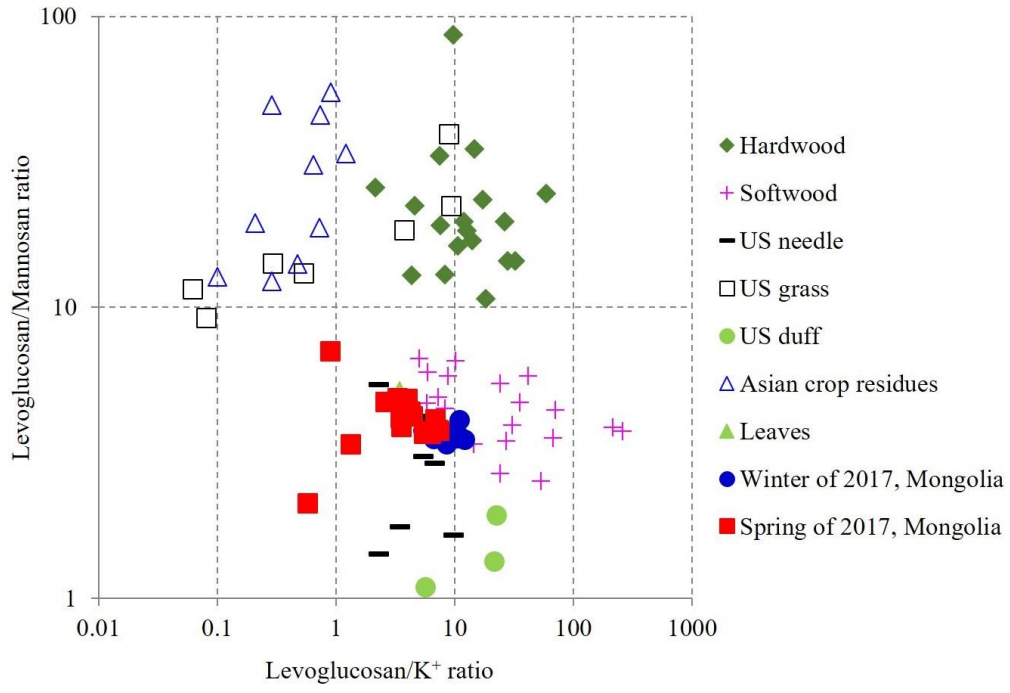
Fig. 9



927
928

929
930

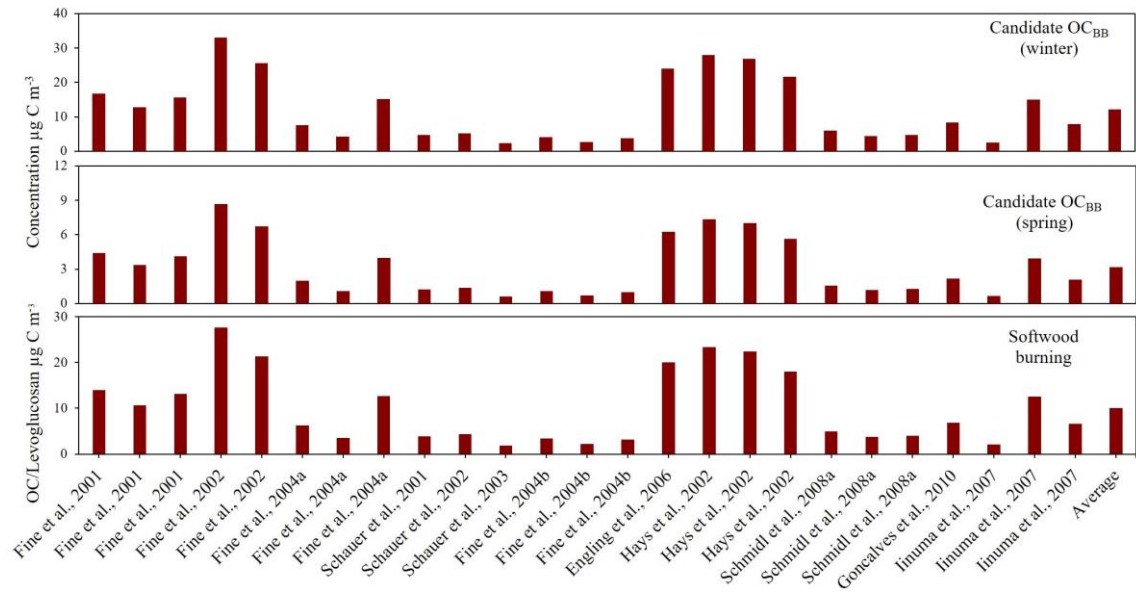
Fig. 10



931
932

933
934
935

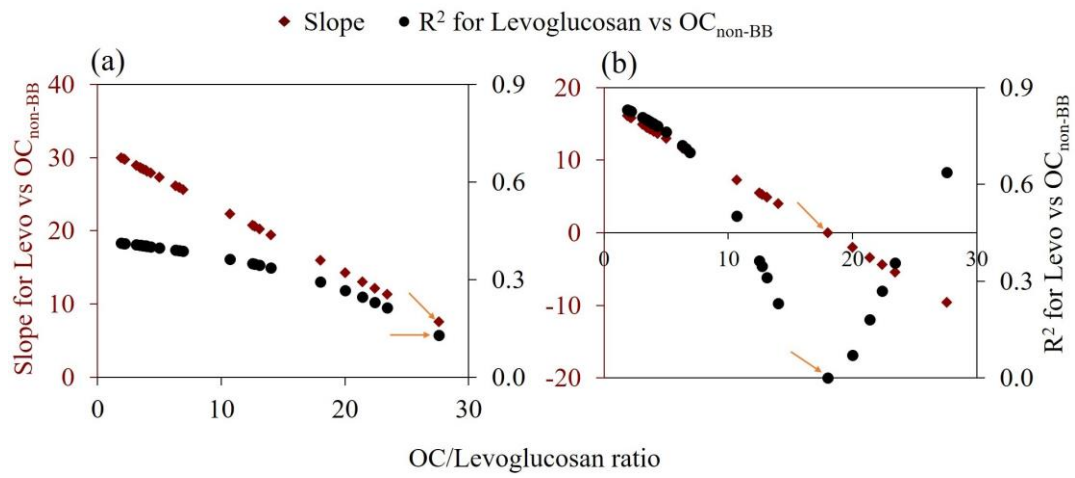
Fig. 11



936
937
938

939
940

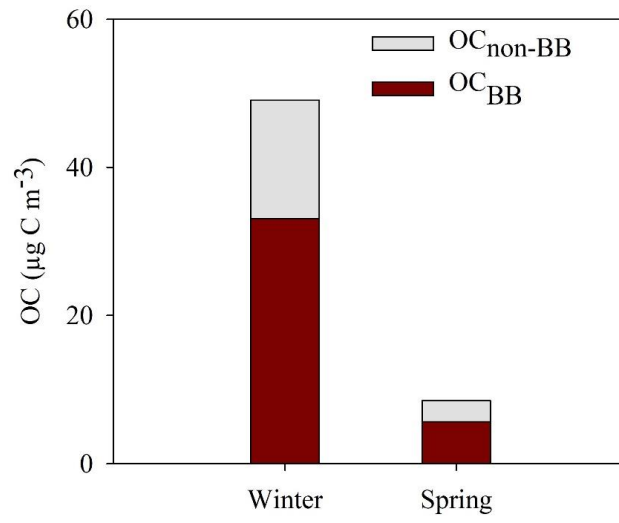
Fig. 12



941
942
943
944
945
946
947
948
949
950
951
952
953
954
955
956
957
958
959
960
961
962
963
964
965
966
967
968
969
970
971
972
973

974
975

Fig. 13



976
977
978